U S

FACULTY OF SCIENCE AND TECHNOLOGY

MASTER THESIS

Study programme / specialisation:
Biological Chemistry

Spring/ autumn semester, 2021

Open

Author:
Priya Vijayaratnam

............Priya Vijayaratnam............
(signature author)

Course coordinator:

Supervisor(s):
Hanne Røland Hagland

Thesis title:

OCT1 expression in pancreatic cancer cell lines MIA PaCa-2 and Panc-1 after metformin and phenformin treatment

Credits (ECTS): 60

Keywords:

Pancreatic cancer
Panc-1
MIA PaCa-2
Metformin
Phenformin
Flow cytometry

Pages: 60

+ appendix: 16

Stavanger, Desember 2021

List of content:

1.Abstract

Pancreatic cancer is the 13th most common types of cancer and has a poor prognosis of survival. Therefore, it is important further investigate different drugs, especially already well-establish medicaments response in regard to treatment for this particular cancer type. The well-established diabetic type II drugs metformin and phenformin are metabolic drugs that can and may be used for cancer treatment. Cancer cells alter their metabolism in order to support their rapid proliferation, whereas both metformin and phenformin makes metabolic changes that causes stops the cancer cell growth process, mainly by their ability to cross the cell membrane. Organic cation transporter 1 (OCT1) are one of the biomarkers being linked to metformin and phenformin import into the tumor cell. The aim for this thesis is the assess both the toxicity, as well as assessing the OCT1 expression when pancreatic cancer cells are being treated with metformin and phenformin.

A dose repose assay was conducted for two pancreatic cancer cell lines, MIA PaCa-2 and Panc-1. The Cell counting kit -8 (CCK8) assay was conducted with different concentration of metformin and phenformin, as well as a rapid response and slower response (6 hours and 24 hours). Although the assay did not give concluding values, it shows implementing changes. Assessing OCT1 expression using flow cytometry gave no clear expression of OCT1 in both cell lines and the aim shifted to troubleshoot both the protocol and theory, before further conduction drug treatment. Both by assessing other biomarkers which are important in tumorigenesis, Akt and AMPK, and the staining using propidium iodine.

2. Abbreviations

ADD Adenosine diphosphate

Akt Protein kinase B

AMPK Activated protein kinase

ASF Amphiphilic solute facilitator

ATP Adenosine triphosphate

CCK-8 Cell counting kit

FSC Forward scatter channel

HK II Hexokinase II

HIF-1 Hypoxia – induced factor 1

IRS Insulin receptor substrate

mTORC1 rapamycin complex 1

OCT Organic cation transporter

OXPHO Oxidative phosphorylation

PI3K phosphoinositide 3-kinase

REDD1 regulated in development and DNA damage responses 1

ROS Reactive oxygen species

SSC side scatter channel

TSC2 tuberous sclerosis complex protein n2

3. List of figures

Figure 8.3.4.2 – *Dot plots from gated MIA PaCa-2 cells with parameter forward scatter (FSC-A and APC-A) for flow cytometry experiment of fixated and permeabilized MIA PaCa cells with added propidium iodine (PI) 19.09.21*

Figure 8.3.4.3 – *Dot plots from gated Panc-1 cells with parameter forward scatter (FSC-A and APC-A) for flow cytometry experiment with fixated and permeabilized Panc-1 cells 19.09.21*

Figure 8.3.4.4 – *Dot plots from gated MIA PaCa-2 cells with parameter forward scatter (FSC-A and APC-A) for flow cytometry experiment of fixated and permeabilized Panc-1 cells with added propidium iodine (PI) 19.09.21*

Figure 8.3.4.5 – *Schematic overview with dot plots and histogram for optimalization of fixated MIA PaCa-2 cells*

4. List of tables

5. Introduction

5.1 Pancreatic cancer:

Cancer is a term used to describe a group of diseases that involves the involvement of abnormal cell growth, having the ability to spread or invade to other parts within the body. Pancreatic cancer is as its name suggest a cancer found in the pancreas, characterized by the formation of malignant cell in. the tissues of the organ (1). Additionally, it is worth mentioning that pancreatic cancer is a general term that consist of several types and can be divided into further sub-types. It is globally the 13th most common type of cancer, known to have a poor prognosis for survival. Age- adjusted incidence rates range from 10-15 per 100,000 people in part of North, Central and Eastern Europa to less than 1 per 100,000 in areas of Africa and Asia (2, 3).

5.1.2 Risk factors

Variables associated with an increased risk of developing pancreatic cancer are risk factors and are mostly collected through observational studies. In the *Textbook of pancreatic cancer: Princicples and Practice of Sugical Oncology (2021)* Søreide and Ståttner has presented different factors that are known to initiate and/or trigger the formation of abnormal cell growth in the pancreas. Current research suggest that age is the most established predictor of pancreatic cancer incidence and death as the risk are low in the first three to four decades of life and have a significant sharp increase after age 50 years, with most patients between the age of 60 and 80 years. Furthermore, evidence from meta-analyses and pooled analyses suggests that having chronic and hereditary pancreatitis are high risk factors to develop pancreatic cancer, representing approximately 5-10 % of all pancreatic cancers (4)

Another factor that has been documented with pancreatic cancer is the consumption of tobacco. Multiple studies suggest that long-term smoking is the most associated risk factor, leading to approximately a double increase of developing the disease. The miscoding and activation of oncogenes are initiated from carcinogens that forms electrophilic compounds, thereby reacting with nitrogen and oxygen atoms within the DNA (5). Several studies have postulated that pancreatic malignancies may be induced through the long-term administration of tobacco -specific N-nitroamines or the paternal administration of other N-nitroso compounds.

Obesity is another risk factor associated with an increased risk of several cancers, including pancreatic cancer, as excess body fat cause changes in the body such as long-lasting inflammation, high levels of insulin and insulin-like growth factors (6). Previously conducted studies indicate that many pancreatic cancer patients were already diagnosed with hyperglycemia or diabetes prior to developing pancreatic cancer. There is no current research that documents that hyperglycemia leads to pancreatic cancer, and vice versa. However, studies have postulated that the development of hyperglycemia may be an early sign of pancreatic cancer, thereby illustrating this diagnose as a tumor enhancer. (7).It has been documented that pancreatic cancer may be responsible for new-onset diabetes, however in the long run prolonged diabetes contributes to cancer progression. (7). Even if there is trouble understanding the correlation between pancreatic cancer and hyperglycemia is has been documented that the overall risk of pancreatic cancer in individuals with diabetes is almost doubled (8). This correlation further supported by finding from biomarker studies(9). Several observational studies suggest that insulin has a prominent role in pancreatic carcinogenies, since prediagnostic elevation of plasma glucose, serum and plasma glucose, insulin(10) (11)and plasma C-peptide levels(12) have been associated with higher percentages of risk(13-15).

5.3 Cell lines

5.3.1 MIA PaCa-2

MIA PaCA-2 is a human pancreatic cell line which is used as a model of pancreatic cancer and was derived from the pancreas adenocarcinoma of a 65-year-old male.

5.3.1 Panc-1

Panc-1 is a human pancreatic cell line isolated from a pancreatic carcinoma of ductal cell origin. The cells can metastasize i.e. pathogenic agents that can spread from an initial or primary site to a different or secondary site within the host´s body (9).

5.3.3. Angiogenic potential for both cell lines

Angiogenesis is defined as the process in which cancerous cell induce proliferation of endothelial cells leading to subsequent formation of new blood vessels. This is essential for both tumor growth and metastasis.

Expression of pro-angiogenic cytokines, chemokines, enzymes and their product are used to assess the angiogenic potential of PA cell lines, and there are different factors being expressed for both the cell line. Not detectable COX-2 protein expression is common for them both, meaning non promotion of converting arachidonic acid into bioactive molecules. PANC-1 displays variable relative expressions of other pro-angiogenic factors, and MIA PaCa-2 displayed consistently low levels of pro-angiogenic factors (9).

5.4 Biomarkers

The term biomarker describes a molecular change in a biological molecule that has arisen from attack by reactive oxygen, nitrogen or halide species.

Biomarkers yield information on three progressive levels to disease outcome:

(i)   Measurable endpoints of damage to proteins/amino acids, oxidized lipids, oxidises DNA bases

(ii)   Functional markers of e.g., blood flow, platelet aggregation, or cognitive function

(iii)   Endpoints related to specific disease (16)

5.4.1 OCT1

The organic cation transporter OCT1 with gene symbol SLC22A1 belongs to the amphiphilic solute facilitator (ASF) family of integral transmembrane proteins.(17) It is primary located in the hepatocytes, even if it has a broad tissue distribution in humans. OCT1 has been located at the sinusoidal membrane and also expressed in cholagiocytes. It is also important to notice that it has been expressed at the basolateral membrane of enterocytes where it accounts together with the combined transport activity of carriers localized at the apical membrane of these cell the secretion of organic cations toward the intestinal lumen. (18)

The human gene SLC22A1 encoding OCT1 is localized within a cluster on chromosome 6q26 and comprises 11 exons and 10 introns. The protein contains 554 amino acids and consist of a 12 alpha- helical transmembrane domains (TMDs) with N-and C-terminals localized in intracellular position. (19)

5.4.2 Regulation of OCT1 expression and function

The regulatory mechanisms of OCT1 expression and function are important, since they can alter the disposition of endogenous substrates or drugs.

This can be categorized by OCT1´s role in the uptake of drugs targeted to hepatocytes, its role in drug efflux from hepatocytes to blood, in the detoxication of cationic drugs, uptake of antitumor drugs and its role of interactions among OCT1 substrates in liver pharmacology.

For this thesis it is the uptake of drugs targets to hepatocytes, where the high expression level of OCT1 at the sinusoidal membrane of hepatocytes accounts for the relevance of this transporter in the handling of many cationic drugs by the liver, which include both metformin and phenformin. OCT1 do obtain a large binding pocket, which has specific domains for different substrates[20]. By being polyspecific, OCT1 can mediate the cellular uptake of many different drugs and can be involved in cellular drug toxicity [18]. As mention above, the OCT1 drug toxicity in liver and also kidneys are well studied, there is a lack regarding pancreatic drug toxicity and OCT1 expression [21] [20]. Additionally, OCT1 promotes organic cations to traverse the blood-brain barrier in the brain and encourage the uptake of endogenous substrates and antiviral drugs in human immune cells. [19]

5.5. Glucose metabolism in cancer cells

Cancer cells alter their metabolism in order to support their rapid proliferation and expansion across the body[22]. Normal cell proliferation in tissues is controlled by the availability to growth regulation factors and by the interaction with surrounding cells. The distribution of nutrient and oxygen for cell proliferation and metabolism is acquired through blood circulation. Initial growth of tumor takes place when there is an absence of formation of new blood vessels, and cells ignore the environmental growth – controlling constraints. [23] Tumor cells exhibit high level of glycolysis despite the presence of ample oxygen, a phenomenon termed as aerobic glycolysis, which was first observed and published by Warburg in 1924 and thereby referred to as the "The Warburg effect". Warburg further proposed that the defects in energy metabolism may be the root of cancer.[24] As cancer research and its genetic basis further bloomed in the 1980s, the understanding of changes in tumor glucose metabolism became viewed as secondary events. This is an important discovery of the molecule involved in the adaptation to hypoxia- induced factor 1 (HIF-1). HIF-1 is a pleotropic transcription factor that regulates genes involved in the hypoxia-induced metabolic switch, regulation of tumor pH and angiogenesis. [25]
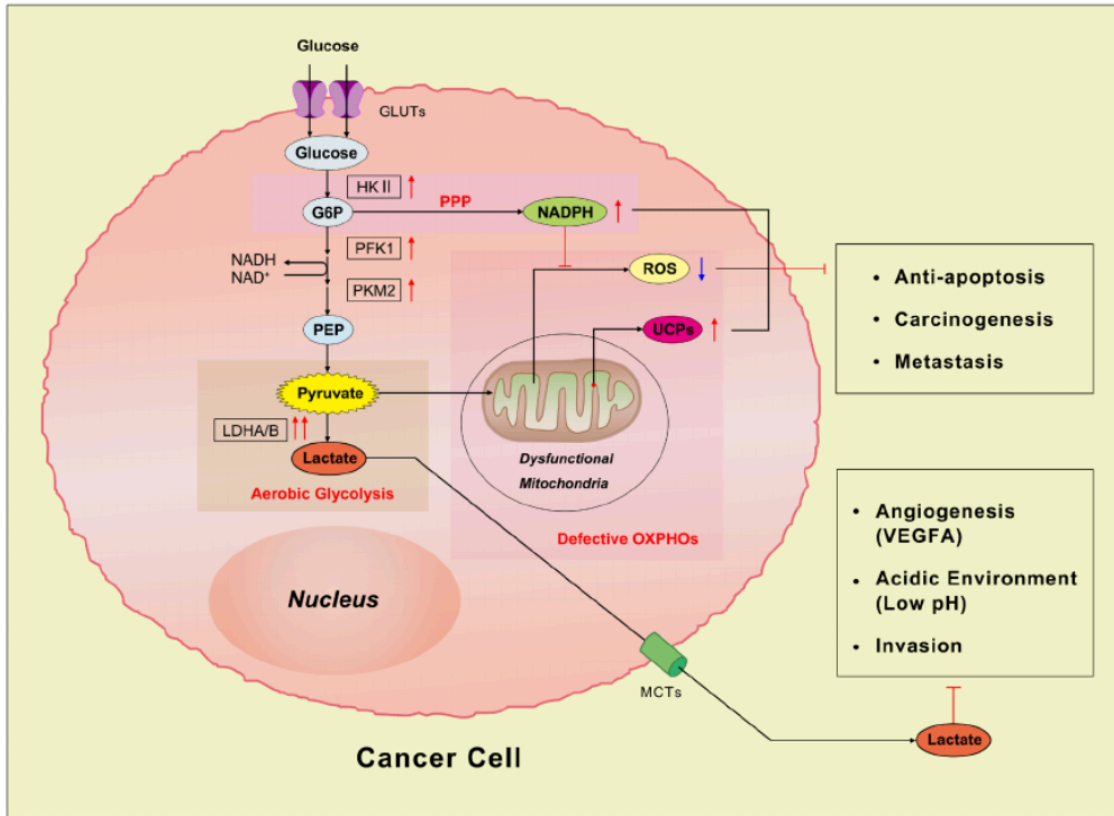
Figure 5.1– The Warburg effect in cancer cells

Figure is obtained from article "The reverse Warburg effect is likely to be an Achilles´ heel of cancer that can be exploited for cancer therapy" by Fu, Yaojie, et al. from the journal Oncotarget, 8 (34), 57813 (open access by creative common attribution) and show that even if the presence of sufficient oxygen, the malignant cell prefers to produce ATP via glycolysis instead of oxidative phosphorylation (OXPHOs), and mainly induces by mitochondrial dysfuntion.

Hexokinase II (HK II) is a known transcriptional target of HIF-1 and catalyze the first step in the glycolic pathway where glucose is phosphorylated to glucose-6-phosphate with conversion of one ATP to ADD. Glucose metabolism can be modulated by having an increase of the expression level of HK II, this from hypoxia via HIF-1. (25)

5.5.1 AKT

There are several drive forces additional to hypoxia that contributes to abnormal glycolytic flux in cancer cells. Over the last years it has been discovered that oncogenes found in a broad variety of human cancer cells may directly activate HIF-1 and other components without hypoxia, one of them being Akt. Akt is a serine/theoserine kinase regulates factors involved in glucose metabilsm and is involved in several cellular processes such as proliferation, autophagy and cell metabolism. It is termed as the "Warburg kinase" and can promote changes in tumor cells and creating a more malignant state. (26)

Akt promotes a glycolytic change under normaoxia conditions, (27)oxygen tensions between 10-21%, without it affecting the rate of oxidative phosphorylation. Confirming that this occurs both as an adaption to low-oxgyen flux and when tumoral cells increase the production of metabolic intermediates required for rapid proliferations, e.g. pentose phosphate for nucleic acid synthesis.

5.5.2 Activated protein kinase (AMPK)

 Another important molecule in regard to disruption of metabolism/ growth control contribution to tumorigenesis is AMP-activated protein kinase (AMPK). AMPK is a highly conserved sensor of low intracellular ATP levels that is rapidly activated after nearly all mitochondrial stresses. When the change between the ATP and AMP ratio occurs, AMPK is activated and phosphorylates downstream targes to redirect metabolism towards an increased catabolism and decreased anabolism. This molecule is composed of an alpha catalytic kinase subunit and a beta -and gamma- regulatory subunit (28). The current model for AMPK activation suggests that when intracellular ATP levels drops and AMP level rises, AMP will directly bind to nucleotide-binding domains in the AMPK gamma subunit, thereby causing a conformational change in the AMPK heterodimer and exposing the activations loop of the catalytic alpha kinase subunit, which may as occur during nutrient depravations or hypoxia.

The canonical AMP – dependent mechanism of activation requires the upstream kinase LKB1, which has been identified to be a tumor suppressor. Increases of Ca^{2+} can also activate the formation of AMPK by glucose starvation and by DNA damage via non-canonical AMP-independent pathways. In regard to cancer, genetic studies suggest that before the disease arises, AMPK act as a tumor suppressor by enhancing AMPK activators such as the biguanide

phenformin. Once the formation of cancer has started, AMPK switches to being a tumor promoter by enhancing cancer cell survival by protecting against metabolic, oxidative and genotoxic stress. (29)

5.6 Metformin

Metformin is the one of the most commonly used drugs for treatment of type 2 diabetes, but yet its primary focus of action remains to be documented. (30)

Its major effects in the human body are to decrease hepatic glucose output, this being especially gluconeogenesis from L-lactate, and to increase both glycolytic lactate production by the intestine and insulin-dependent peripheral glucose utilization. As mention previously the prevalence of diabetes gives a higher risk (risk factor) of pancreatic cancer, as well as cancer in liver, endometrium, breast, colon, rectum and urinary bladder compared to individuals without this chronic disease. It is worth mentioning that the results of extensive epidemiologic studies repeatedly indicates that diabetes type II patients that have receive metformin, compared to those taking other antidiabetic medication, had a decreased risk of the occurrence of various types of cancer (31) (32) (33).

5.6.1 Molecular action of metformin in cancer cells

The current proposed anticancer action of metformin is mainly with the inhibition of rapamycin complex 1 (mTORC1). As discussed before about the Warburg effect, it was though for many years that it was a result of mitochondrial damage. However, in recent years there are significant progress in this understanding and that cancer cells do have a functional mitochondrion. mTORC1 participate in the regulation of mitochondrial ATP producing capacity which affects tumor cells. TOR is a large serine/threonine protein kinase that belongs in the family of phosphoinositide 3-kinase (PI3K) – related kinase and interacts with other proteins and form two distinct multiproteins complexes, mTOR Complex 1 being the one inhibited by rapamycin. (34) Several evidence suggested that the inhibition of mTOR pathways by metformin proceeds dependent and independent on AMP-activated protein kinase (AMPK) activation. AMPK phosphorylates tuberous sclerosis complex protein n2 (TSC2) that inhibits mTORC1 leading to decrease in protein synthesis and cell growth. (35)

5.7 Phenformin.

Phenformin is also a biguanide hypoglymic agent with actions and uses similar to those documented of metformin.(36) Through the years, the synthesis of metformin has led to the development of the compound phenformin and buformin. However, these derivatives were withdrawn from the marked in the 1970s due to their lipophilic structure that give them a high affinity for mitochondria membranes to interfere with oxidative phosphorylation and cause latic acidiois (37).

Phenformin is nearly 50 times as potent as metformin, but due to its association with higher lactic acidosis which caused its withdrawn from clinical use of effect on phenformin on cancer has rarely been studied. The reason phenformin is more potent than metformin is due to the way it enters into the cells. Metformin is a very hydrophobic compound and requires organic cation transporters (OCTs) to pass through the cellular membrane, whereas phenformin does not need any transport proteins to enter. This means that it permits a higher concentration of phenformin inside the tumor cells, but also achieves successful treatment in tumors with no OCT overexpression.
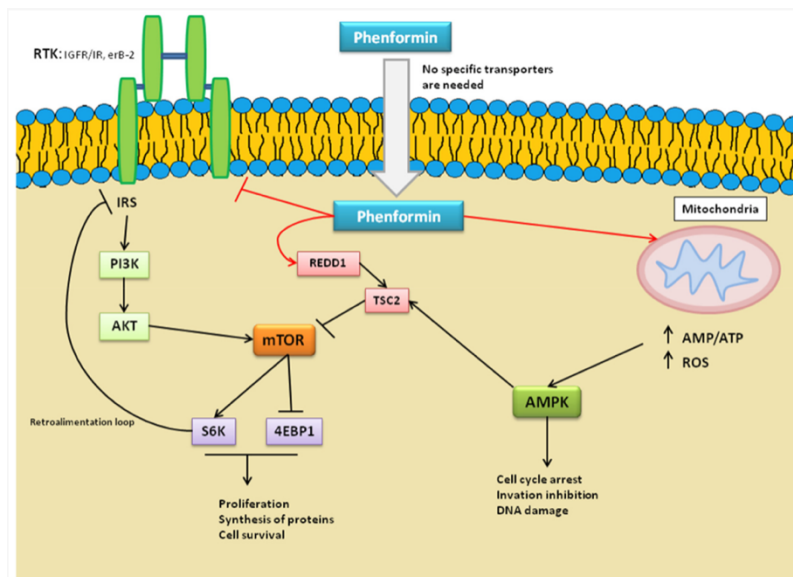
Figure 5.7 – Mechanism of Action of Phenformin

Figure is obtained from article "Phenformin as an Anticancer Agent: Challenges and Prospect" from the International Journal of Molecular Sciences 20 no.13:3316 and illustrates the different ways phenformin acts when it passes though the cellar membrane.

When phenformin passes freely through the cellular membrane it acts in three different ways (illustrated in **Figure 5.7**) :

1) Inhibits the complex I of the mitochondrial respiratory chain
2) Activation of REDD1 protein
3) Inhibits insulin receptor substrate (IRS) receptors which leads to AMP-activated protein kinase with energy detection (AMPK) activator and mTOR pathway blocking (discussed previously). This process leads to cell cycle arrest, invasion inhibition and DNA damage.

Compared to metformin, phenformin has a higher antitumor effectiveness due to its higher absorption level inside the tumor cells and its higher potency and tissue bioavailability (37).

6. Aim of the thesis

Metformin and phenformin are metabolic drugs that may also be used for cancer treatment, as it relays in their ability to penetrate (and cross) the cell membrane. Organic cation transporter 1 (OCT1) has been linked to metformin and phenformin import in the tumor cells. This project aims to establish OCT1 expression in two pancreatic cell lines (MIA PaCa-2 and Panc-1) before and after drug exposure.

Main objectives to be resolved are:
- To assess the effect of metformin and phenformin drugs in cancer cell lines of pancreatic cell lines MIA Paca-2 and PANC-1 in terms of toxicity responses
- To assess whether the OCT1 expression is influenced by metformin or/and phenformin treatment as a function of time and concentration (6-hours and 24 hours, acute and long – term effects) in MIA PaCA-2 and PANC-1 using flow cytometry.

7. Material & Methods

7.1 Materials

Table 7.1 - Chemical used

Chemical	Supplier	Catalogue/ Lot. Nr #
AlamarBlue	VWR	MFCD0005036
Propodium Iodine	Sigma-Aldrich	P4864
Fixative Solution (4% formaldehyde prepared in PBS)	Invitrogen by Thermo Fisher Scientific	20H285301
Flowclean Cleaning Agent	Beckman Culter	A64669

Table 7.2 - Cell lines & Antibodies

Name	Supplier	Catalogue #
MIA PaCa-2	ECACC General Collection	ECACC 85062806
Panc-1	ATCC	MFCD000005036
SLC22A1 antibody	GeneTex	GTX80400
CF® 4888A Llama Anti Mouse IgG	Biotium	18C0821
CF 488A IgG Llama anti-rabbit	Biotium	16C1128
Akt (pan) Rabbit mAb	Cell signaling technology	10/2017
AMPK-alpha Rabbit	Cell signaling technology	07/2017
P-akt (S473) Rabbit Ab	Cell signaling technology	03/2017
P-AMPK (40H9) Rabbit Ab	Cell signaling technology	10/2017

Table 7.3 -Reagents for cell culture

Chemicals	Supplier	Catalogue #
DMEM (Dulbecco´s Modified Eagle´s Media) without glucose, L-glutamine and sodium pyruvate	Corning	17-207-CV
Foetal Bovine serum, heat inactivated, South America origin	Biowest	S181H-500
Penicillin: Streptomycin solution 6,0/10,0g/L 100 X	Biowest	L0022-100
L-glutamine, 200 mM	Corning	25-005-Cl
Trypsin EDTA 1X	Corning	25-053-Cl
PBS tablets	ThermoFisher	189112-014

Table 7.4 - Commercial kits and reagents

Name	Supplier	Catalogue #
Cell Counting Kit-8	Tebu-bio	CK04-05
Muse® Count & Viability kit	Luminex	B86303

Table 7.5 - Equipment & Software

Name	Supplier
Cytoflex flow cytometer	Beckman Coulter Inc.
Muse^{TM} Cell analyzer	Luminex
SpectraMax ® Paradigm® Multi-Mode Microplate reader	Tecan
CytoExpert Software	Beckman Coulter Inc.

7.2 Aseptic technique:

All the following methods and techniques in regard the cultivation of cell culture were conducted according to aseptic technique. Gowns and shoe covers are required for both protection and reducing further debris from the outside. Glows were sterilized with 70% ethanol prior to use. The laminated hood, reagents, bottles and all necessary equipment were being used were also sterilized with 70% ethanol as well as UV decontamination of the hood.

7.3 Resuscitation of frozen cell lines:

Individual cryotubes containing MIA PaCa -2 and Panc-1 cell lines were removed from the cryotank (liquid nitrogen storage), and quickly thawed in a 37ºC water bath for approximately 2 min. The content was then transferred into a pre-warmed growth medium and then centrifuged for standard values (21º, 900rmp, 5 min). The growth medium was evaporated and 10mL of pre-warmed growth medium was again added. These steps were performed in order to remove the toxic amount of DMSO (10%) which the freeze medium contains. The cells were transferred to a new flask and were then incubated at 37ºC with 5% CO_2 in a humidified incubator.

7.4 Cell suspension:

The cell culture flasks were carefully placed under a microscope for assessing contamination and the confluency of the cells. When it was assessed to have no contamination and the level of confluency was ~ 60-70% the culture medium was removed by aspiration. Rinsing with pre-warm 1xPBS (phosphate-buffered saline) and then removed, prewarmed 2 mL X Trypsin – EDTA was added and incubated at 37ºC with 5% CO_2 in a humidified incubator until the cells were detached from the flask. This was around 1 – 2 min, but it was determined by either gently move/rock the flask and looking at cell movement or putting it under a microscope and see the cell culture moving in a more microscopical level.

For Panc-1 pancreatic cell line, which was had highly adherent cultures, this took more than 1-2 min, and would even take 5 min and was checked every minute for sign of detachment. Warm and fresh media was added (10 mL) and the thoroughly mixed by pipetting. This is to make sure of having a suspension of single cells. An appropriate volume of this cell suspension was transferred to a new flask and added more fresh media. The volume

transferred was depended on the split size, growth and demand for cells. Mostly splits were done as 1:2 -1:5 and the change of a new flask after every 10 days.

7.5 Cell Medium:

The composition of cell culture media is described in **Table 7.5.**

Table 7.5 – DMEM Complete media with low glucose

Components	Volume (mL)
Dulbecco´s Modified Eagle´s Media without glucose, L-glutamine and sodium pyruvate	500
Fetal bovine serum, heat inactivated (South American origin)	50
Penicillin: Streptomycin solution 6.0/10.0g/L 100X	10
L-glutamine, 200 mM	10
Glucose solution (2,5M)	1,1

7.6 Harvesting and cell counting – Muse Count and Viability assay

To harvest the correct needed number of cells for further assays the use of Muse^{TM} Cell Count and Viability assay was used, which is a rapid and reliable alternative to trypan blue exclusion. It provides absolute cell count and viability data on cell suspension from a variety of cultured mammalian cell lines. Viable and non-viable cells are stained based on their permeability to the two DNA binding dyes present in the reagent.

- The DNA-binding dye in the reagent stains the cells that have lost their membrane integrity, allowing the dye to stain the nucleus of viable and non-viable cells.

- A membrane – permanent DNA staining dye that stains cells with a nucleus. The Muse ^{TM} System counts the stained nucleated events and determine an accurate total cell count by distinguish free nuclei and cellular debris from cells[38].

After treatment with trypsin and addition of fresh cell growth media as explained in section 7.3 and a small amount of cell suspension is transferred to a 1,5 mL Eppendorf tube. 1,5 mL microcentrifuge tubes especially used for the Muse^{TM} Cell analyzer instrument are then filled with appropriated amount of Muse^{TM} Count & Viability reagent (See table below for amounts mL used). Cell suspension is added to the microcentrifuge tube. The tube with both the cell suspension and reagent is mixed well by vortex and incubated for 5 min at room temperature before being loaded into the Muse^{TM} Cell analyzer instrument.

Table 7.6– Cell suspension dilution table

Concentration of original cell suspension (cells/mL)	Dilution factor	Cell suspension volume (µL)	Count & Viability reagent volume (µL)
1×10^5 to 1×10^6	10	50	450
1×10^6 to 1×10^7	20	20	380
1×10^7 to 2×10^7	40	20	780

Each plot given in the Muse^{TM} Cell analyzer has moveable markers, that gives the opportunities to eliminate debris based on size and have a moveable threshold marker that eliminates non-nucleus cells. The plot also has an angle marked that allowed to separate viable cells from dead cells. By having such a visual plot presented, it was easy to observe if the cell culture has been cultivated properly or if the confluency had reached a non-useable point.

The viability values during all the assays preformed have been preferred to be between 98,5 – 99 % consistently, with the default number for event to acquire is 1000. (39)

7.6 Determine the cell density – AlmarBlue ®assay

AlamarBlue ®monitors the reducing environment of the living cells. The active ingredient is reazuring (40), a water-soluble compound that is stable in culture medium and is non-toxic and permeable through cell membranes. This gives a continuous monitoring of cells in culture. The dye acts as an intermediate electron acceptor in the electron transport chain without interfering of the normal transfer of electrons. (41)

AlamarBlue® is an oxidized blue non-fluorescent dye that when accepted is reduced to the pink-colored, high fluorescent resorufin. This change from an oxidized to reduced state allows flexibility of detection where measurements can be quantitative as colorimetric and/or fluorometric readings. The oxidation-reduction potential is +380 mV at pH 7,0 in room temperature. It is safe to say that it functions as a cell health indicator using the reducing power of living cells to the conduct assays for measure the proliferation in cell lines(42).

Mia PaCa- 2 and Panc-1 cell cultivated in cell flasks were harvested and determined cell count by using the Muse^{TM} Count & Viability assay as described above and the cell suspension was then normalized to contain different densities. (5×10^5, 10×10^5, 20×10^5 , 25×10^5, 30×10^5 and 35×10^5). To a 96 well plate, both cell lines as well as positive control(resorufin) and untreated media were added in parallels and with a final volume of 100 μL in each well. The cultured cells were stored at 37ºC in a cell culture incubator for 24 hours. Added 10 μL aseptically of 484 μM AlamarBlue reagent to the untreated media as well as the different parallels with cells suspension at different densities. In the well with positive control, 10 μL of ultrapure sterile water was added. The 96 well plate was incubated for 4 hours in the cell incubator at 37ºC.

After incubation the plate was read by a SpectraMax ® Paradigm® Multi-Mode Microplate reader to measure the fluorescence values at excitation wavelength at 540 nm and emission wavelength at 590 nm. Since AlamarBlue® is a reagent that slowly converts into fluorescents product over time when exposed to light, the plate was wrapped in a layer of aluminum foil when transported from the incubator to the reading instrument.

7.7 CCK8 assay

Cell counting kit -8 allows convenient assay by utilizing Dojindo´s water-soluble tetrazolium salt. WST-8 [2-(2-methoxy-4-nitrophenyl)-3(4-nitrophenyl)-5-(2,4-disulfophenyl)-2*H*-tetrazolium, monosodium salt] produces a water-soluble formazan dye upon reduction in the presence of an electron mediator.
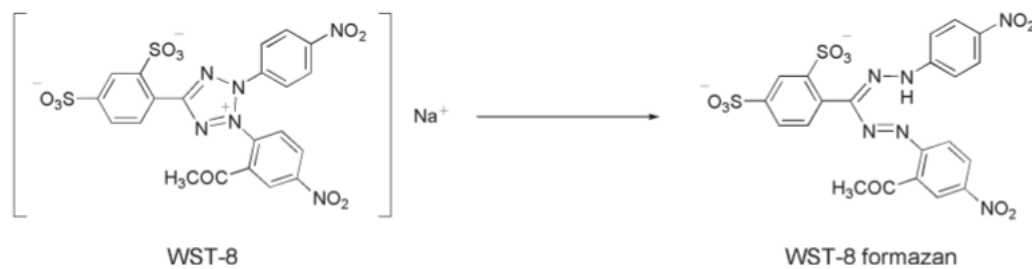
Figure 7.7.1 - Structures of WST-8 and WST -8 formazan. *Obtained from Cell Counting Kit-8 Cell proliferation Assay and Cytotoxicity Assay Dojindo Laboratory CK04*

CCK-8 allows sensitive colorimetric assays for the determination of the number of viable cells in cell proliferation and cytotoxicity assays being nonradioactive. WST-8 is reduced by dehydrogenases in cells to give an orange-colored product, this being formazan. It is soluble in the tissue culture medium, and the amount of the formazan dye generated by dehydrogenases in cells is directly proportional to the number of living cells.

This principle of the cell viability detection for CCK-8 is shown in **Figure 7.7.2** below.
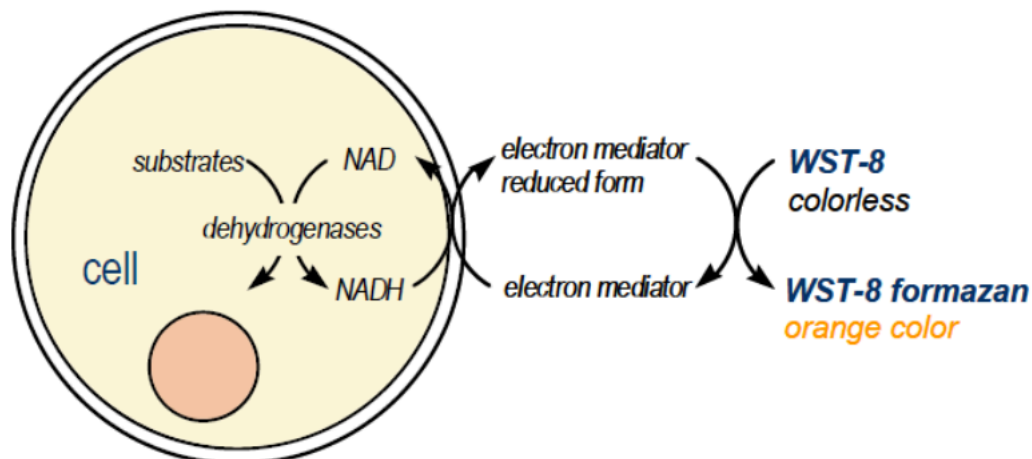
Figure 7.7.2 – Principle of the cell viability detection with CCK-8 *Obtained from Cell Counting Kit-8 Cell proliferation Assay and Cytotoxicity Assay Dojindo Laboratory CK04*

Mia PaCa- 2 and Panc-1 cell cultivated in cell flasks were harvested and determined cell count was determined by using the Muse^{TM} Count & Viability assay and added 100 µl of cell suspension with 1 15* 10^5 cells per well of Panc-1 and MIA PaCa-2 with 25* 10^5 cells per well in a 96-well plate and pre-incubated for 24 hours (37°C, 5% CO_2)

Aspirated away media and added 110 µL of following concentrations presented in **Table 7.7.1,** as well as parallels with: untreated control (only media) and positive control (media + 0,02% DMSO). The plate outline is presented in Table 7.7.1

Table 7.7.1 – Stock solution and added concentration of metformin/phenformin for CCK-8

	Stock solution	Added concentrations						
Metformin	250 mM (in H₂O)	8000 µM	4000 µM	2000 µM	1000 µM	500 µM	250 µM	100 µM
Phenformin	200 mM (in DMSO)	2000 µM	1000 µM	500 µM	250 µM	100 µM	50 µM	25 µM
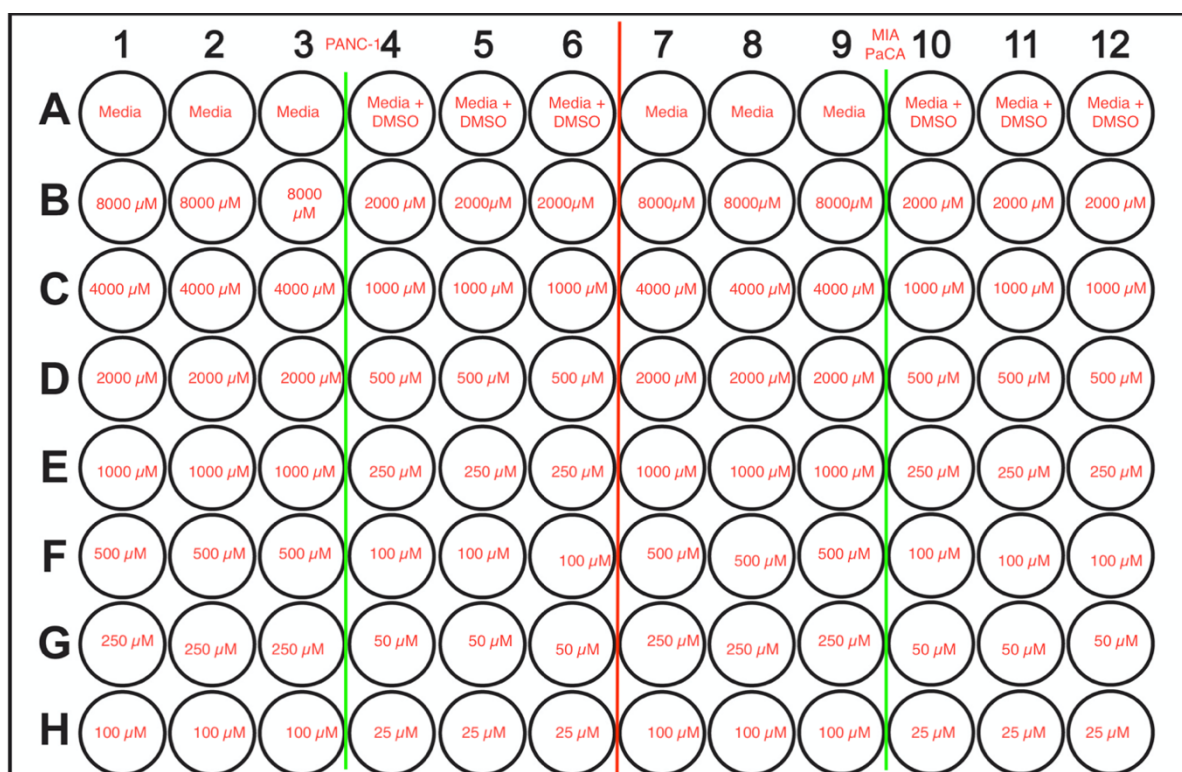
Figure 7.7.3 – Schematic overview of the plate set-up for CCK-8 with PANC-1 and MIA PaCa-2

Cancer cell lines PANC-1 and MIA PaCa were exposed to compounds metformin and phenformin for 6 and 24 hours with various concentrations as shown in Table 7.7.1

Incubated the 96 well- plate for either 24 hours or 6 hours (37°C, 5% CO_2). After the incubation period 10 µl of CCK-8 solution was added to each well and further incubated for 2 hours. After incubation the plate was read by a SpectraMax ® Paradigm® Multi-Mode Microplate reader to measure the absorbance at 450 nm. The plate was covered in a layer of aluminum foil from transferring from the incubator to the reader instrument.

7.8 Flow cytometry

7.8.1 Principals of flow cytometry:

Flow cytometry is a technique used to both detect and measure the properties of individual particles. In this process a sample consisting of cells or/and other particles is injected into a flow cytometer where they are randomly distributed in 3D-space. The sample must therefore be ordered into a stream of single particles that can be interrogated by the machine´s detection system, which is managed by the fluidics system. This system consists of a central channel where the sample is injected, and which is enclosed by an outer sheath that contains faster flowing fluid. When the sheath fluid moves (in this experiment the sheath fluid is ultrapure water) it creates a massive drag effect on the narrowing central chamber. The velocity of the central fluid is altered, and the flow front becomes parabolic with greatest velocity at its center and zero velocity at the wall. This creates a single file of particles and is called hydrodynamic focusing, and without this the nozzle of the instrument would be blocked and makes it impossible to analyze one cell at the time.

After the hydrodynamic focusing, each particle is passed through one or more light beams. The light scattering or fluorescence emission provides information about its properties. Forward scatter channel (FSC) is light that is scattered in the forward direction, normally 20 °C offset from the laser beams axis and collected by a lens. FSC intensity roughly equates to the particles size and are also used to distinguish between cellular debris and living cells. Side scatter is light measured approximately at 90° angle to the excitation line. The side scatter channels (SSC) gives information about the granular content within a particle. (43)

7.8.2 Fixation

The required amount of cell from Mia PaCa- 2 and Panc-1 cell cultivated in cell flasks for further analyses was harvested and determined by using the Muse™ Count & Viability assay as described in sections 7.5. The cell suspension was set to 1 million cells/mL. To obtain a cell pellet, the appropriate amount of cell suspension was transferred to a centrifuge tube and centrifuge at standard values (900 rmp, 21ºC and 5 min).

After removing the supernatant, the cells were resuspended in 100 ul. 4% formaldehyde per million cells. It is important to mix well by resuspending up and down 10 -15 times to dissociate the pellet completely and prevent cross-linkage of individual cells, and to reduce shear pressure a 1 mL pipette is used. The cells were fixed for 15 min in room temperature. Proceeded to permeabilization step, but if there were necessary to run the flow cytometry analyzing the next day, cells were stored overnight in 1XPBS.

The removal of formaldehyde was done by washing by centrifugation with excess 1 xPBS (900 rmp, 21ºC and 5 min). The supernatant was discharge in a safe container for and tossed in an appropriate biohazard waste bucket, since formaldehyde is highly toxic. Resuspended cells in 1 X PBS and stored at 4ºC.

7.8.3 Permeabilization

Removed formaldehyde as described above and resuspended the cells in ice cold 90% methanol (v/v in 1X PBS) by gentle vorexing drop by drop. The cells were then permeabilized on ice for 10 min and proceed to immunostaining. If there were necessary to run the flow cytometry analyzing the next day, the cells were stored at -20ºC in 90% methanol.

7.8.4 Immunostaining:

Aliquoted desired number of cells in 9 Eppendorf tubes for the two cell lines:
For Mia PaCa -2 is $2,5*10^5$ cells and Panc-1 is $1,5*10^5$ cells were respectfully used in each Eppendorf tube for treatment.

The outline of the different Eppendorf tubes was:

Table 7.8.4.1 – Different Eppendorf tubes for Immunostaining

	Treated with:
$\frac{1}{400}$	1/400 of total volume of first primary antibody. Had two parallels
$\frac{1}{200}$	1/200 of total volume of first primary antibody. Had two parallels
$\frac{1}{50}$	1/50 of total volume of first primary antibody. Had two parallels
1º	Only primary antibody
2º	Only secondary antibody
B - Buffer	Only buffer

Centrifuge for 5 min at 10000 rmp, to obtain a clear pellet. Remove supernatant and washed with PBS twice (500 µL). Then it was added the following **(Table 7.8.4.2)** and incubated overnight with rotation in the laboratory cold rom.

Table 7.8.4.2 – Values for immunostaining – primary antibody

	Treated with:	Total volume
$\dfrac{1}{400}$	0,875 µL antibody with BSA-PBS buffer	350 µL
$\dfrac{1}{200}$	1,25 µL antibody with BSA-PBS buffer	350 µL
$\dfrac{1}{50}$	5 µL	250 µL
1º	0,875 µL antibody with BSA-PBS buffer	350 µL
2º	BSA-PBS Buffer	250 µL
B	BSA- PBS Buffer	250 µL

The following day all the tubes washed with 500 µL PBS and centrifuged for 1000 rmp for 5 min. The supernatant is discharged and repeated.

Resuspended in 100 Resuspended cells in 100 µL of:

$\dfrac{1}{400}$, $\dfrac{1}{400}$, $\dfrac{1}{200}$, $\dfrac{1}{200}$, $\dfrac{1}{50}$, $\dfrac{1}{50}$ and 2º Eppendorf tubes with 9,375 µL secondary antibodies with BSA-PBS buffer (in a total volume of 750 µL)

Whereas the Eppendorf tubes containing B and 1º is just resuspended in BSA-PBS buffer. Tubes were incubated with rotation for 1 hour in room temperature and washed twice with PBS. Removed the supernatant and resuspended in 250 µL of PBS for further analyzing. (44)

7.9 Addition with Propidium Iodine:

Propidium iodine (PI) is a fluorescent dye that interscales between bases and stains both DNA and RNA. PI is impenetrable in intact cell membranes and is therefore used for distinguishing viable cell and necrotic cells. PI is excited at 488 nm and emits at a maximum wavelength at 617 nm. The stock solution used is 1 mg/ml and is diluted to 1:1000 in PBS and then immediately added to the cells for further analyzing, instead of resuspended in 250 uL PBS (45) (46).

8. Results

8.1 Determine cell density - AlamarBlue assay

To determine the optimal cell density for further assays AlamarBlue assays was used. The plate outline and values are shown in Appendix. There are some differences in plate outline, this being an optimization with having a positive control. By having them in the outer four corners, it decreased the possibility for sources of error during the plate reading.
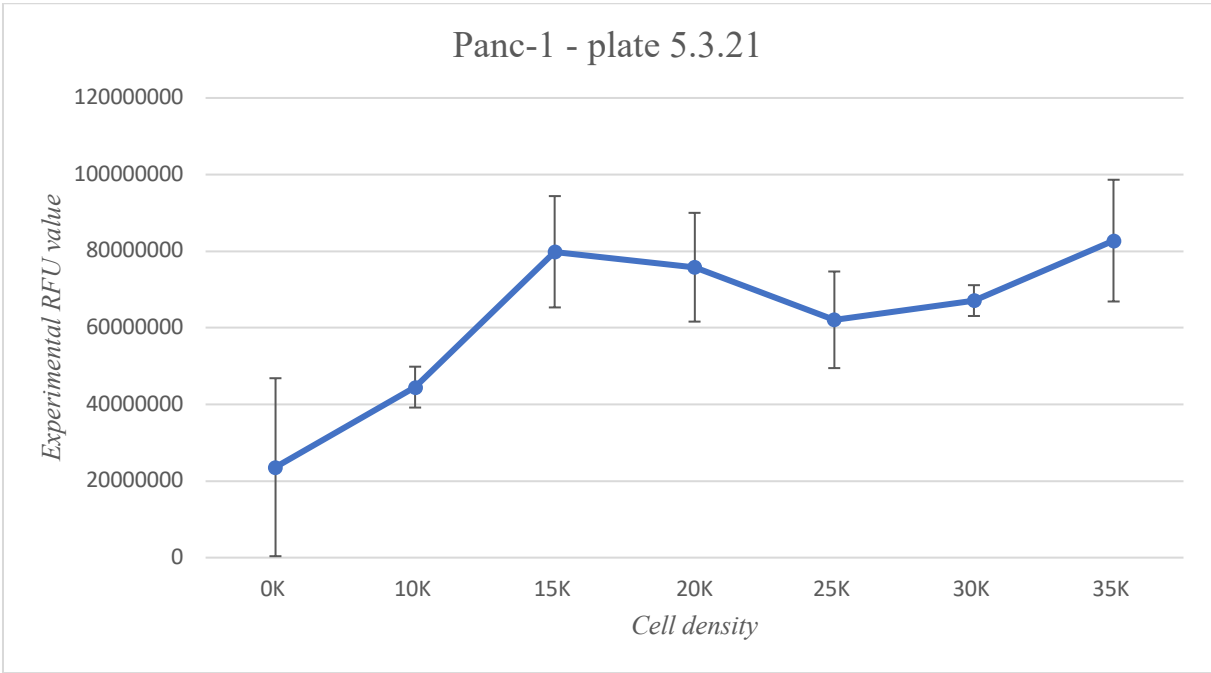
Figure 8.1.1 – Graph of experimental RFU value from different cell density in Panc-1 reading of plate 5.3.21 with standard deviation.
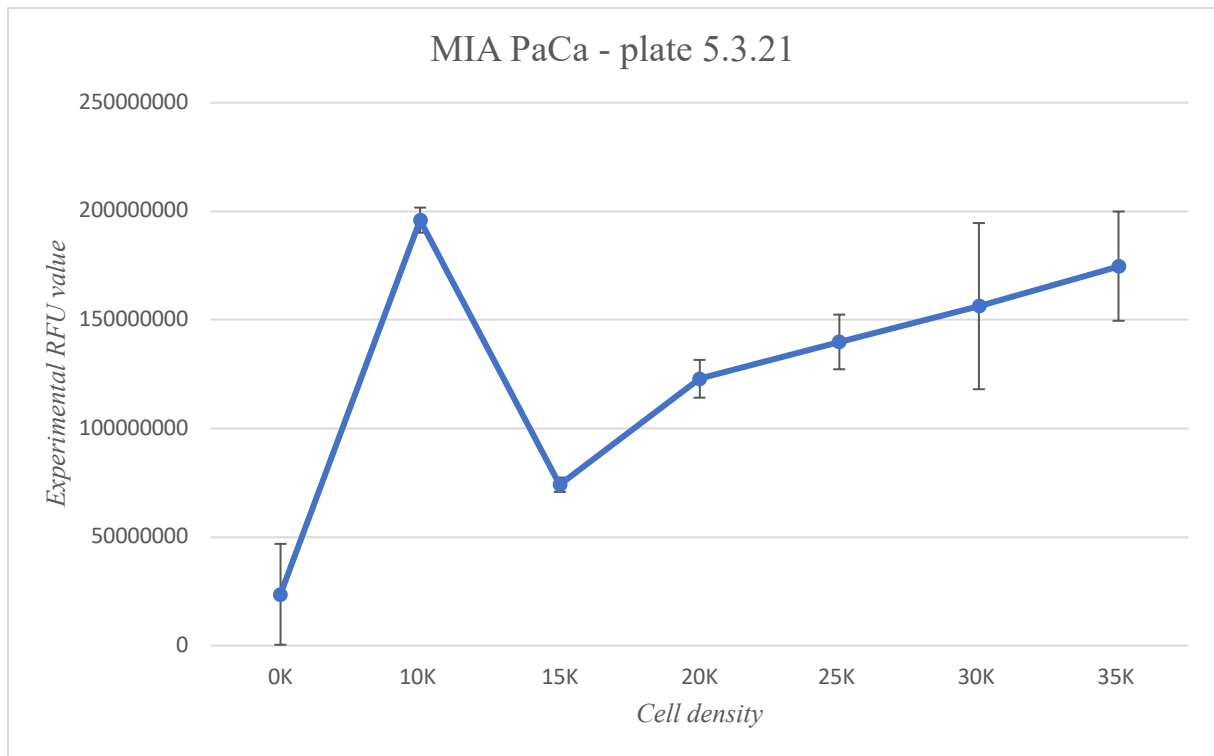
Figure 8.1.2 – Graph of experimental RFU value from different cell density in MIA PaCa reading of plate 5.3.21 with standard deviation.

By looking into the experimental RFU values, **Figures 8.1.1** shows the stabile cell density for Panc-1 to be at 15K cell density Even if the standard deviation values are highest at this point, this is the clear peak. For MIA PaCa-2 the stabile and optimal cell density can be seen at 25 K, even if this is not the highest peak. The curve drops immediately after 10 K and does stabilizes more properly at 25K.

8.2 CCK8

After determining the optimal cell density by AlamarBlue assay (Panc-1 is 15000 cells and MIA PaCa-2 is 25000), CCK8 assays with different concentration of metformin and phenformin was conducted for 6 hours incubation time and 24 hours incubation time. This is to see a change during a rapid treatment and a slower response.
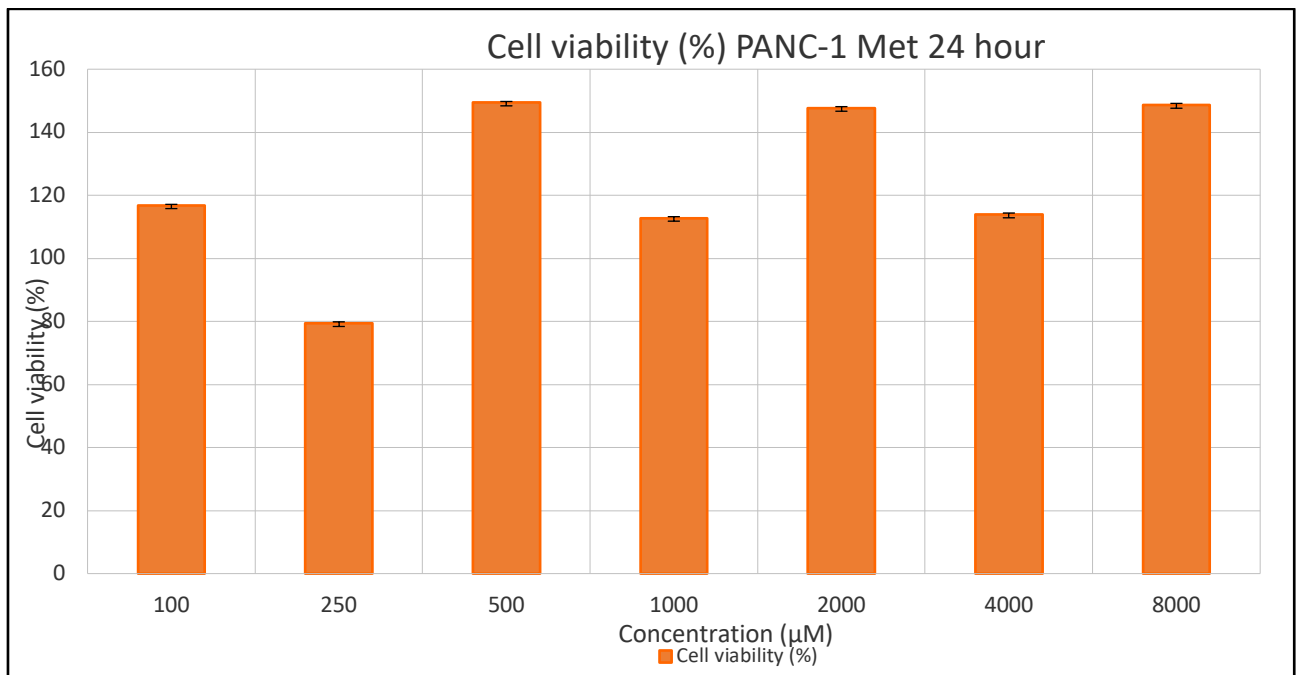
Figure 8.2.1 - Cell viability (%) for PANC-1 cancer cells treated with metformin for 24 hours.
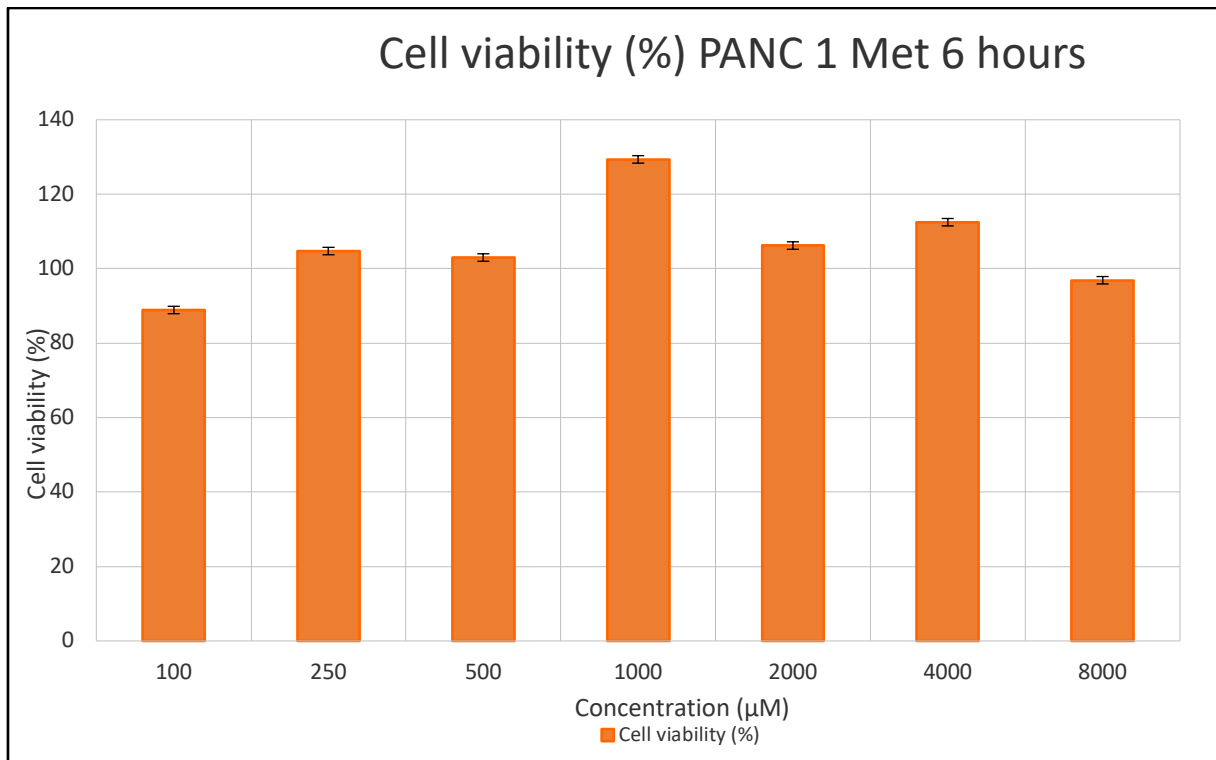
Figure 1.2 - Cell viability (%) for PANC-1 cancer cells treated with metformin for 6 hours.

The cell viability (%) in **Figure 8.2.1** for 24 hour treatment with metformin gives not a clear indicator, where the viability both decrease and increases with the increase of concentration of metformin used for treatment. As for the slower response, this being 6 hours it is the lowest concentration that has the lowest value 88,89 %. However, there is a slight decrease when reaching 8000uM. The cell viability values are normalized with the control and presented in percentages. In both **Figures (8.2.1 and 8.2.2)** the viability percentages increase well over 100%.
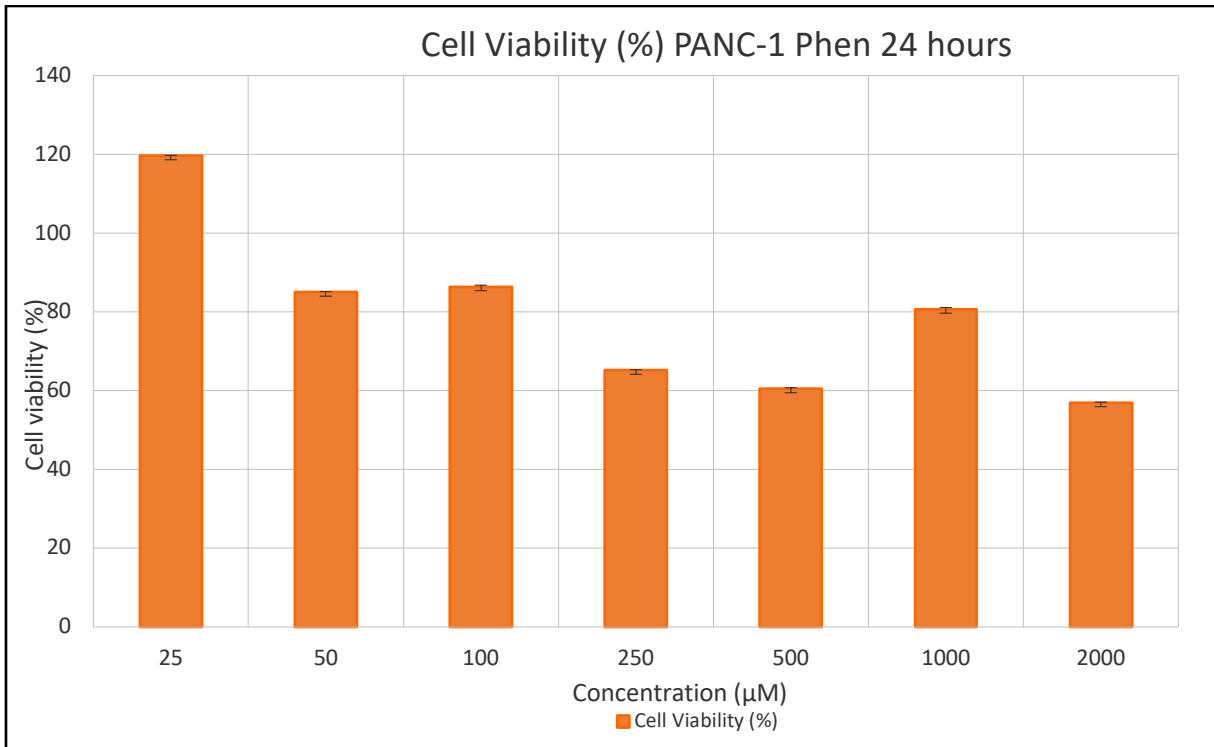
Figure 8.2.3 - Cell viability (%) for PANC-1 cancer cells treated with phenformin for 24hours.
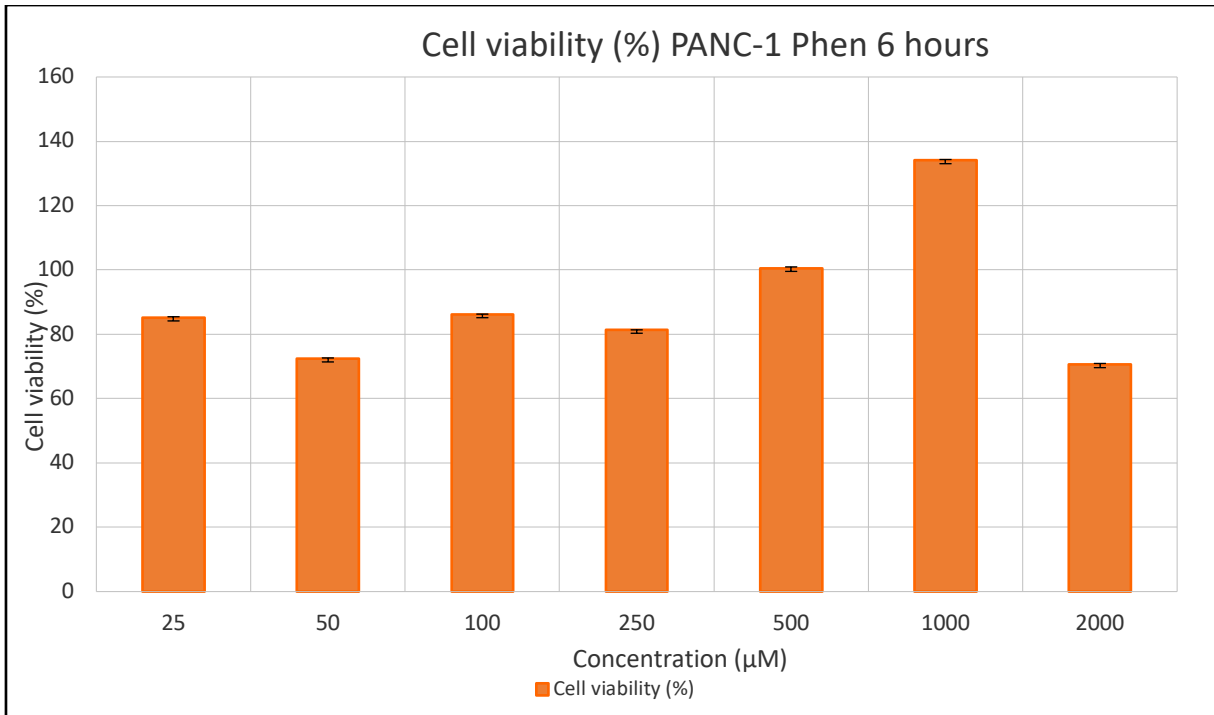
Figure 8.2.4 - Cell viability (%) for PANC-1 cancer cells treated with phenformin for 6 hours.

In contrast to MIA PaCa-2 result regarding metformin treatment, phenformin treatment displays more expected values. Viability percentages decrease significantly while the concentration of phenformin increases in **Figure 8.2.3**. For 6 hour treatment the values do not fluctuates, even if the highest concentration as expected gives the lowest viability (%).   The higher concentrations of phenformin does give a higher yield (lower cell viability (%) overall and this correlates with the notions that phenformin is more potent than metformin.
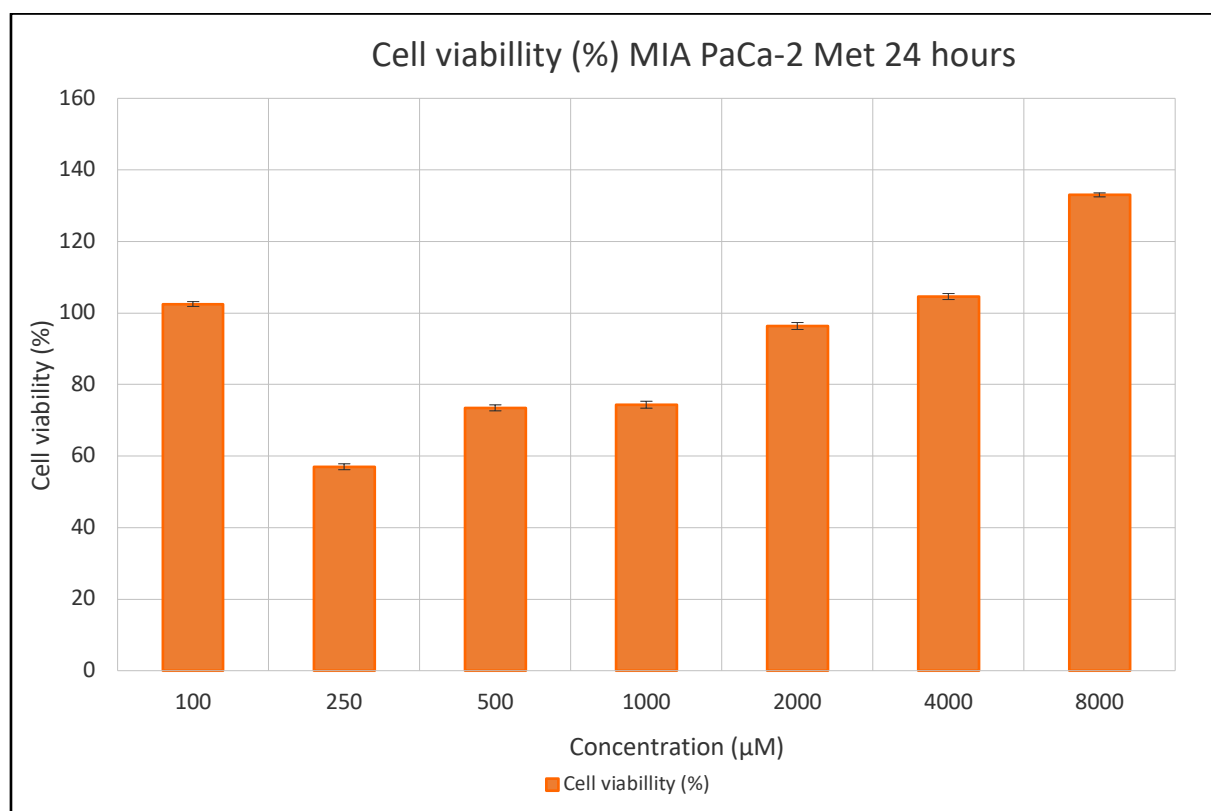
Figure 8.2.5 - Cell viability (%) for MIA PaCa-2 cancer cells treated with metformin for 24 hours.
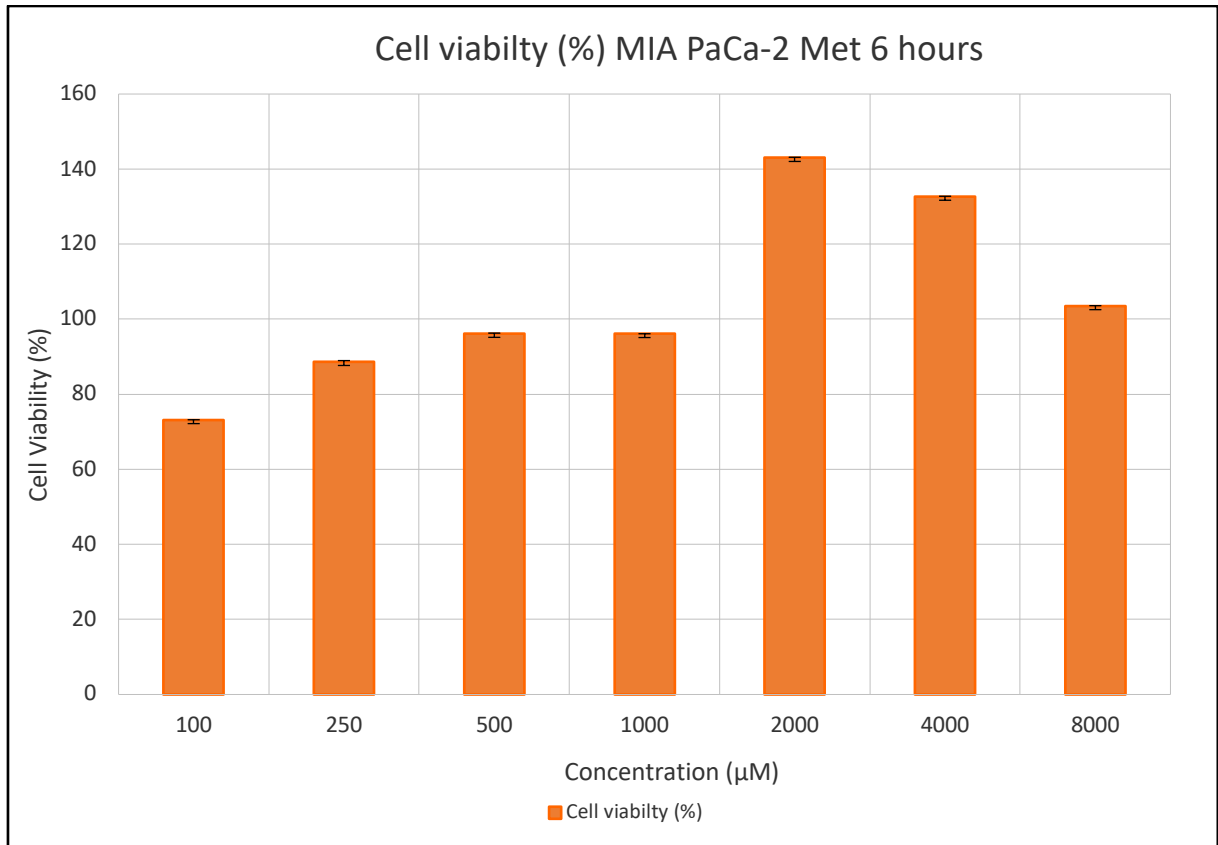
Figure 8.2.6 - Cell viability (%) for MIA PaCa-2 cancer cells treated with metformin for 6 hours

MIA PaCa -2 treament with metformin for both 6 and 24 hours have some unconclusive results. It is the lowest concentration of metformin that gives the lowest cell viability, whereas there is an increase both for the 24 hours and 6 hours treatments when the concentrations get higher. Values obtained from metformin treatment for Panc-1 have a fluctuation, whereas both MIA PaCa -2 and Panc-1 has lowest viability at 100 uM and 250 uM at respectfully for 24 hours and 6 hours responses. This indicates sources of error, since the viability should decrease as the concentration increases.
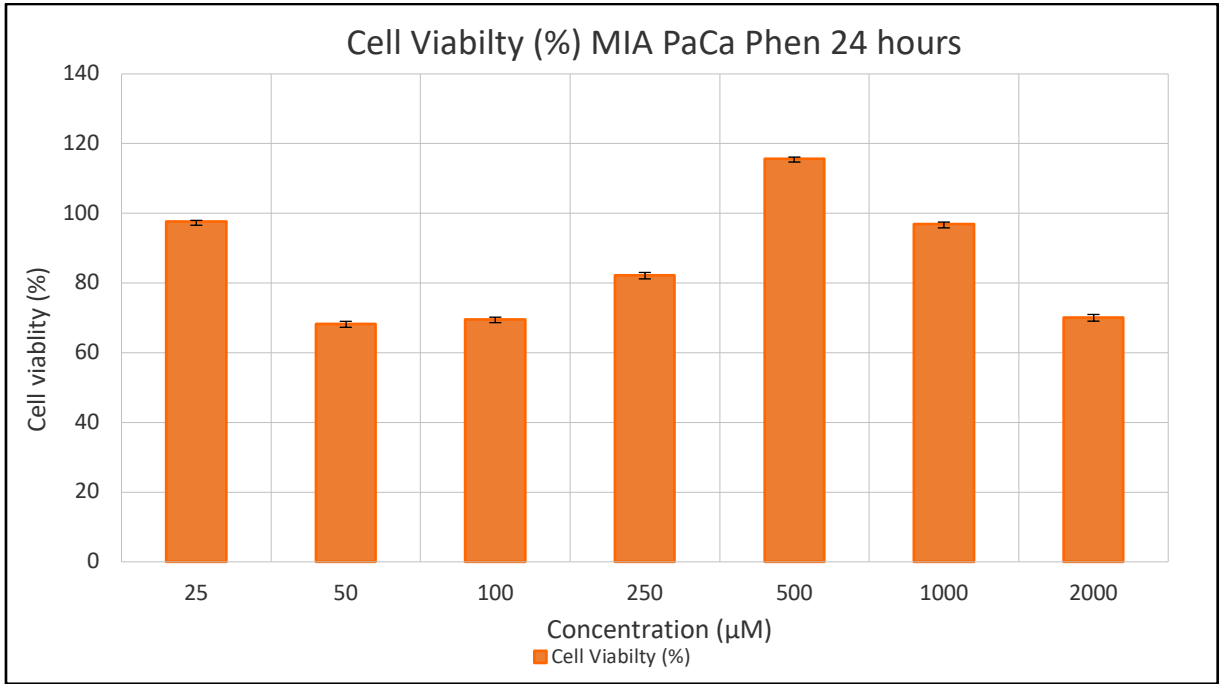
Figure 8.2.7 - Cell viability (%) for MIA PaCa cancer cells treated with phenformin for 24 hours
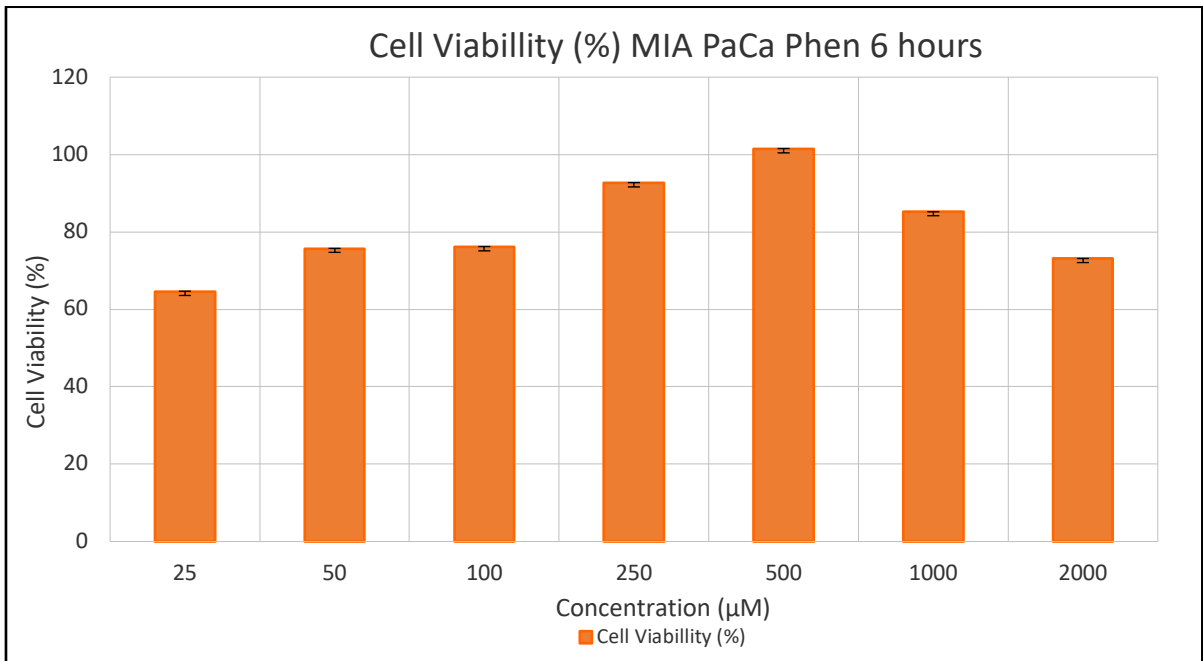
Figure 8.2.8 - Cell viability (%) for MIA PaCa cancer cells treated with phenformin for 6 hours

Treatment with phenformin of MIA PaCa- 2 correlates with Panc-1 values, as in there are significantly a decrease in viability when the concentration increases, even if both figures have a higher peak at 500 uM and then the decrease happens. Both figures are relatively alike and there are just small differences in values, meaning that the time period may not have that huge differences for phenformin treatment in Panc-1 cell line.

8.3 Flow cytometry

8.3.1 OCT1 antibodies – SCCL22

By obtaining values from the CCK8 assays of the cell viability (%) of Panc-1 and MIA PaCa -2 treated with different concentration of metformin and phenformin, the values should be used in flow cytometry analysing of OCT1 expression with treatment. By studying the OCT1 expression, the protein was tagged using primary antibody and a fluorescent secondary antibody. To optimize the concentration of the two antibodies for each cell line, it was preformed dilution experiments of the primary antibody. **Table 8.3.1.1** and **8.3.1.2 is** obtained and calculated data with GeoMean values from both the FITC -A channels, as well as PE-A channel. FITC-A is the channels where it was expecting emission from the secondary antibody, but PE-A channel values are also obtained since there were uncertainty if the emission would be shown in both filters.

Table 8.3.1.1 – Calculated data from executed flow cytometry of permeabilizes MIA PaCa cells 2.06.21 with the GeoMean values from FITC-A and PE-A channel and its standard deviations

	GeoMean FITC-A	GeoMean PE-A	STD. Dev FITC	STV. dev PE
Blank	934,4	1555,4	0	0
1°	759	1349,7	0	0
2°	8115,9	3618	0	0
1:50 u	11040,35	28260,3	2879,7	776,35
1:50 p	12205,75	5034,75	3778,95	670,05
1:200	5297,2	2547,8	542,9	138,4
1:400	4822,5	4598,25	3388,5	849,85

Table 8.3.1.2 – Calculated data from executed flow cytometry of permeabilizes Panc-1 cells 2.06.21 with the GeoMean values from FITC-A and PE-A channel and its standard deviations

	GeoMean FITC-A	GeoMean PE-A	STD. Dev FITC-A	Std.dev PE-A
Blank	927,3	1643,5	0	0
1°	549,6	1130,9	0	0
2°	2363	1767,5	0	0
1:50 u	9954,95	4202,85	5,55	90,45
1:50 p	15231,05	40979,65	2146,85	35754,35
1:200	5579,7	2705,9	221,6	60,6
1:400	7392	3349,2	0	1

Figure 8.3.1.1 – Bar chart of GeoMean FITC-A values presented in Table 8.3.1 & 8.3.2 - Data from executed flow cytometry of permeabilized MIA PaCa cells 2.06.21

Figure 8.3.2.1 – Bar chart of GeoMean PE-A values presented in Table 8.3.1 & 8.3.2 - Data from executed flow cytometry of permeabilized MIA PaCa cells 2.06.21

Histograms and dot-plots for MIA PaCa-2:
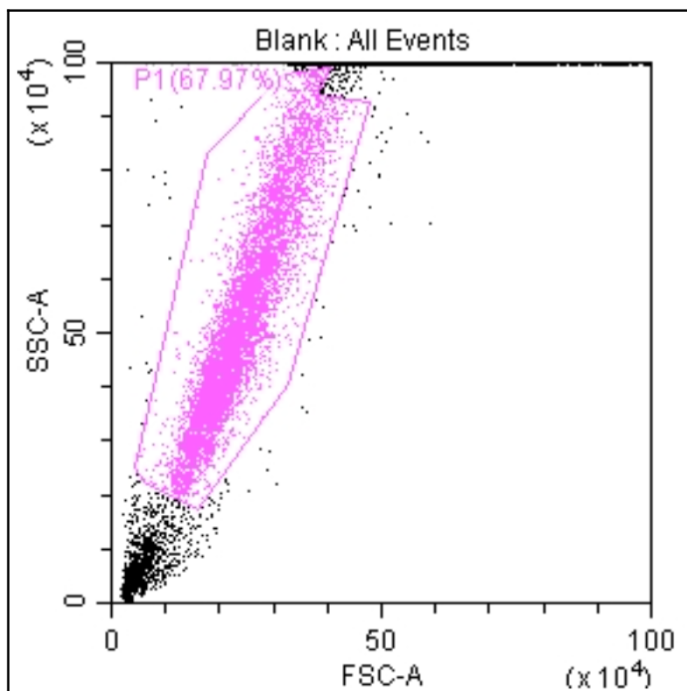
Figure 8.3.1.3 – Gated MIA PaCa cells with parameter forward scatter (FSC-A) for executed flow cytometry experiment for permeabilized MIA PaCa cells 2.06.21
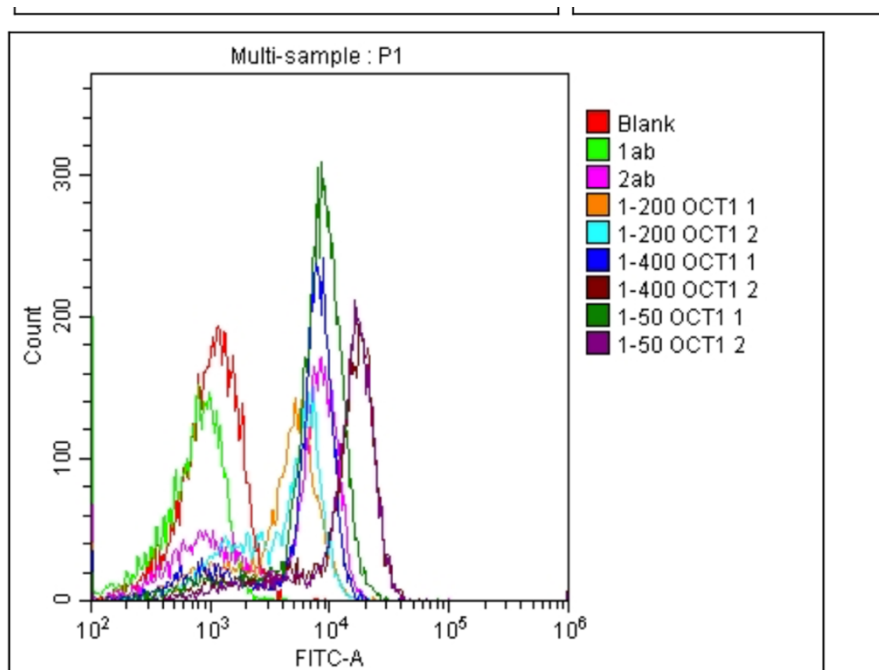
Figure 8.3.1.4 – Overlay histogram for executed flow cytometry experiment for permeabilized MIA PaCa cells 2.06.21 with detection of FITC-A channel for gated area (P1)- from Figure 8.3.1.3
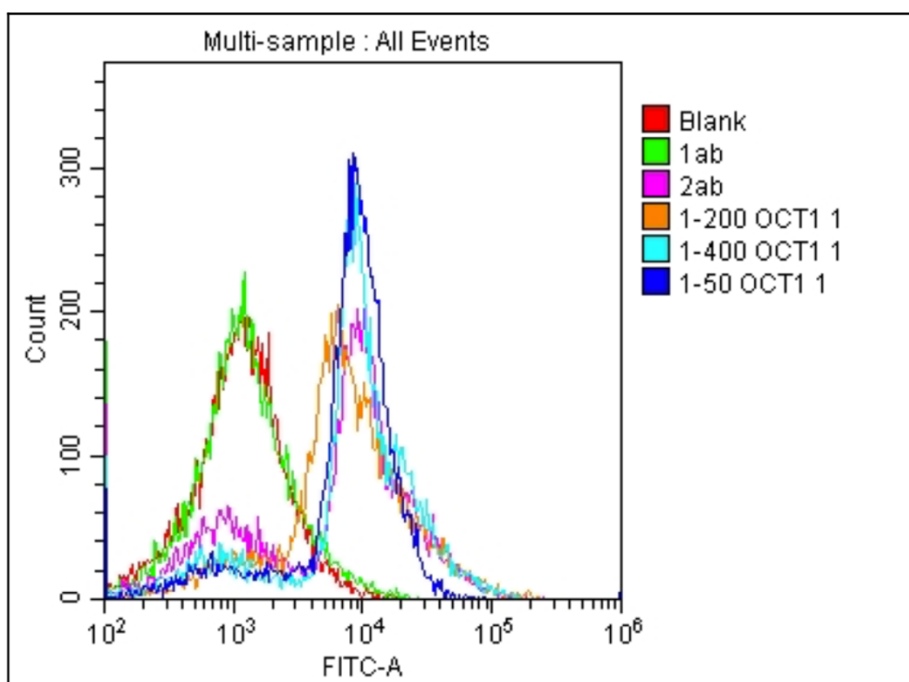
Figure 8.3.1.5 – Overlay histogram for flow cytometry experiment for permeabilized MIA PaCa cells 2.06.21with detection of FITC-A channel for all events with only one titration parallel

Histograms and dot-plots for Panc-1:
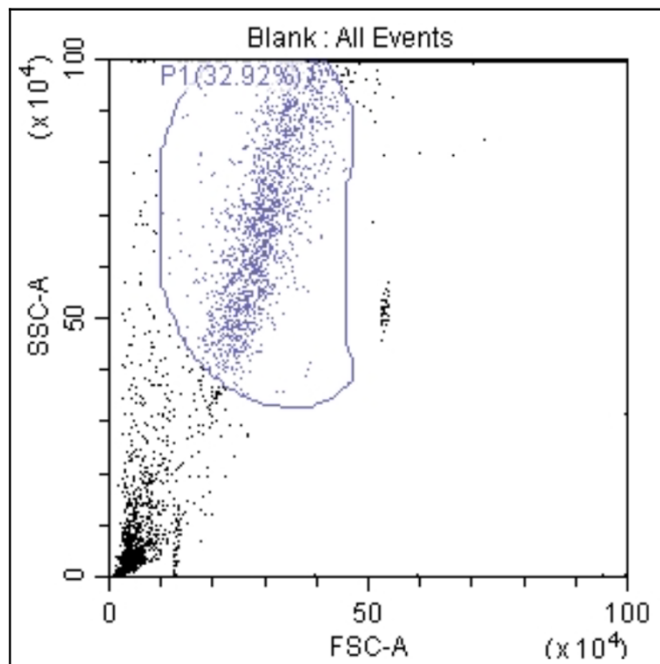
Figure 8.3.1.6– Gated Panc-1 cells with parameter forward scatter (FSC-A) for executed flow cytometry experiment f of permeabilized Panc-1 cells 2.06.2
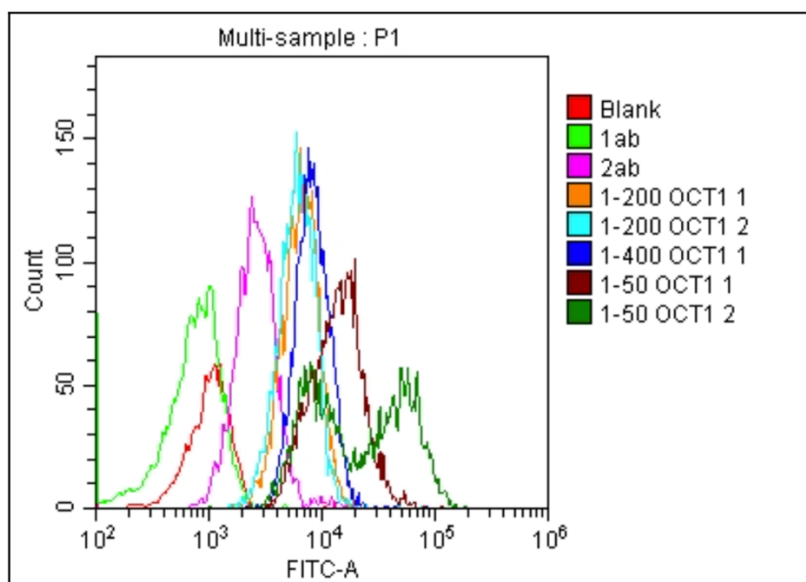
Figure 8.3.1.7 – Overlay histogram for executed flow cytometry experiment of permeabilized Panc-1 cells 2.06.2 with detection of FITC-A channel for gated area (P1) shown in Figure 8.3.1.6
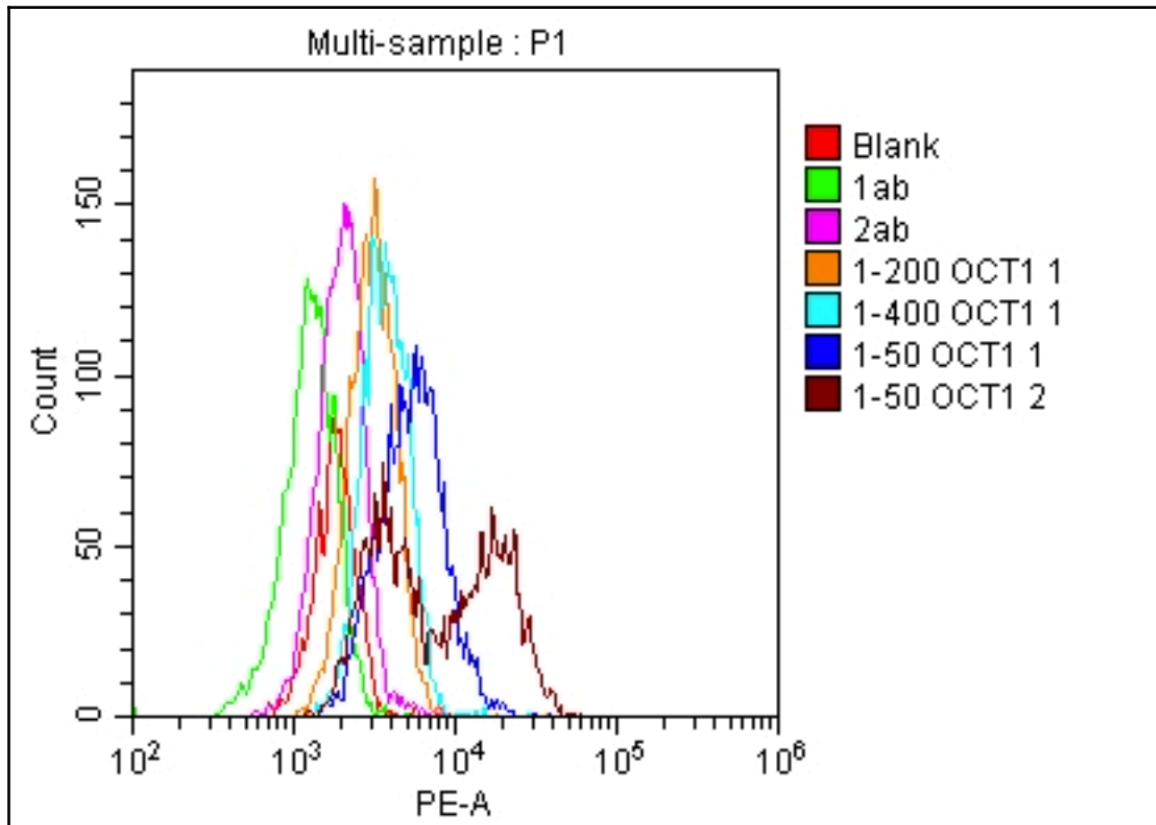
Figure 8.3.1.8– Overlay histogram for flow cytometry experiment of permeabilized Panc-1 cells 2.06.2 titration with detection of PE-A channel for gated area (P1) from Figure 8.3.6 for all events with only one titration parallel

As shown in both histogram for MIA PaCa-2 and Panc-1 both with the gated channel being PE-A or FITC-A, there are a slight clear detectable shift in the curves. This means that there is no strong positive expression of OCT1 in regard to the blank and 2º sample, but some OCT1 could be expressed.

8.3.2 AKT and p-AKT antibodies

Panc-1 and MIA PaCa-2 was treated with antibodies for expression of AKT and p-AKT, hoping it would give a stronger positive expression than the antibodies used for OCT1. Both AKT and p-AKT and its corresponding pathways is influenced by treatment of metformin and phenformin and this correlation is therefore suitable for further examination.

Table 3.2.2.1 – Data from executed flow cytometry of permeabilizes MIA PaCa cells and Panc-1 11.06.21

	Perm 11.06.2021	GeoMean FITC-A
MIA PaCa	Blank	943,1
	2°	6497,3
	Akt	12299,7
	p-Akt	7336,5
Panc -1	Blank	754,8
	2°	4899,3
	Akt	95493
	p-Akt	6583,3
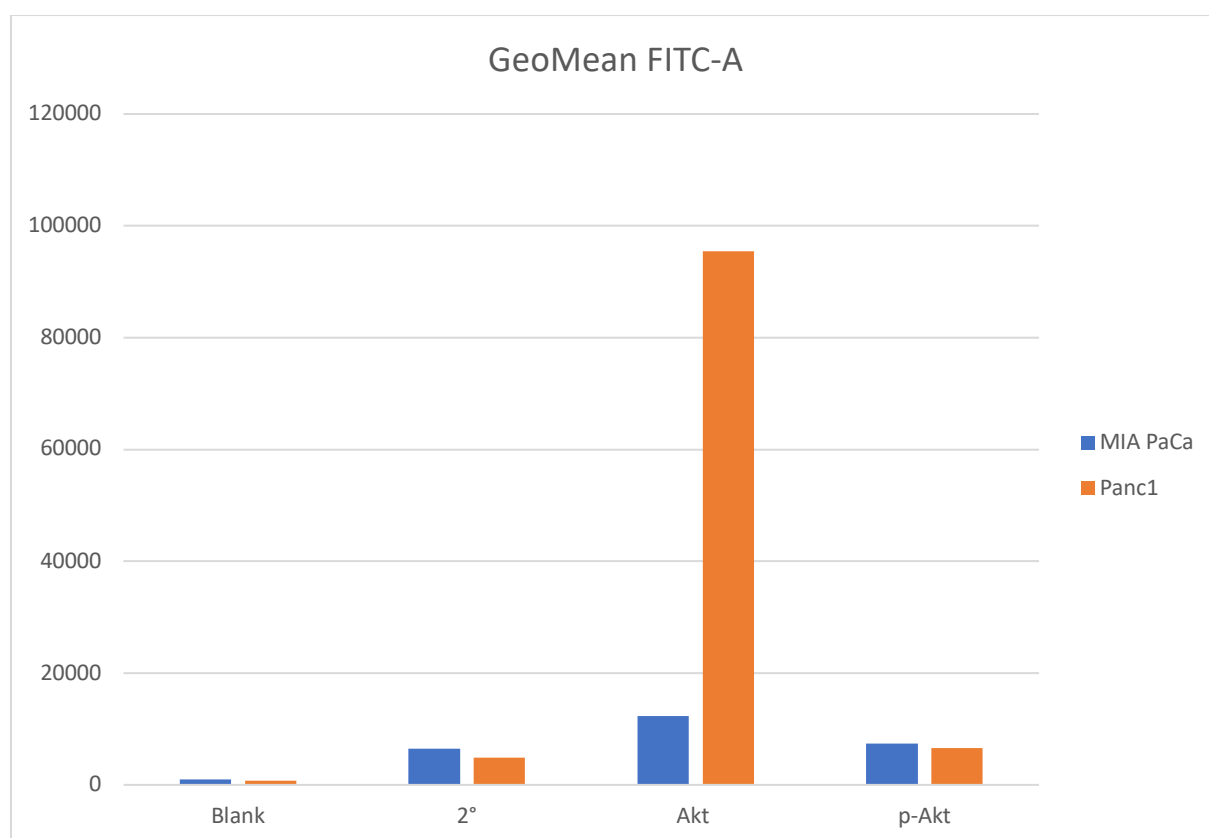
Figure 8.3.2.1 – Bar chart of GeoMean FITC-A values presented in Table 1.1 - Data from executed flow cytometry of permeabilized MIA PaCa cells 11.06.21
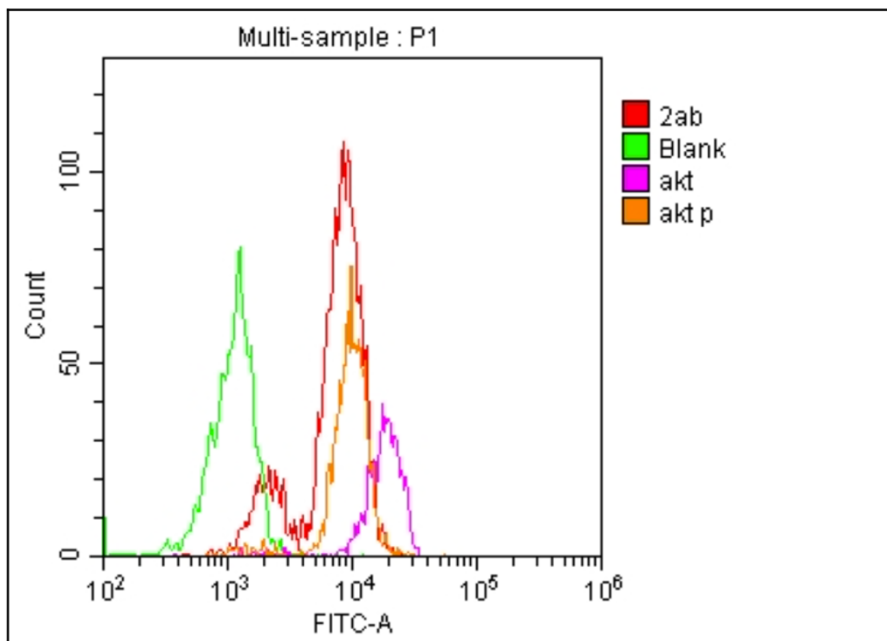
Figure 8.3.2.2 – Overlay histogram for executed flow cytometry experiment for permeabilized MIA PaCa cells 11.06.21 with detection of FITC-A channel for gated area (P1)
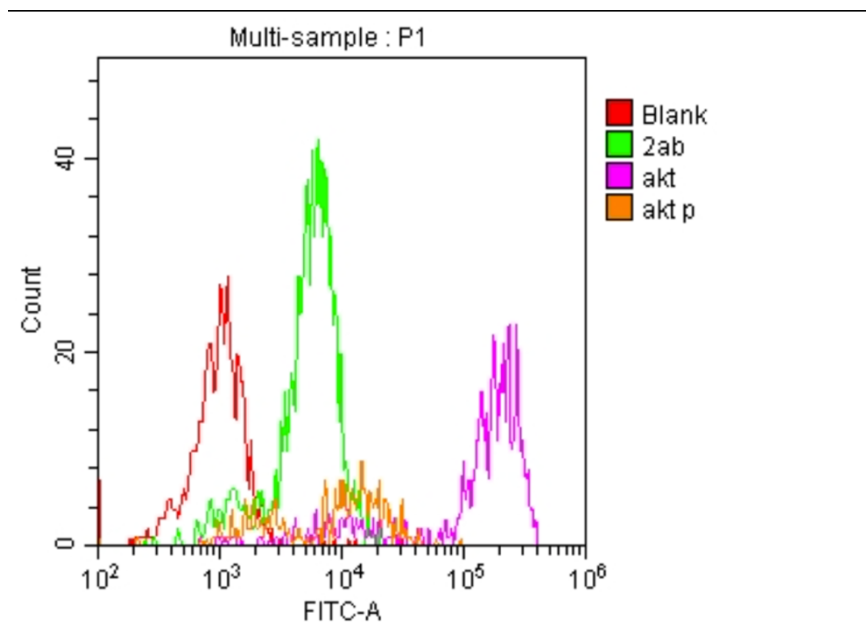
Figure 8.3.2.3 – Overlay histogram for executed flow cytometry experiment for permeabilized Panc-1 cells 11.06.21 with detection of FITC-A channel for gated area (P1)

All the given histograms for permeabilized MIA PaCa -2 and Panc-1 cells in regard to expression of AKT and p-AKT shows expression, with there being a clear shift between the antibodies and 2°.

There are also tendencies that the different curves having a "tail", which indicates not a clean expression and could be a result of contamination and sources of error during the analysing process. As shown for Panc-1 the shift is located in the "noise" area and having a "tail".

8.3.3 AMPK and p-AMPK

To test for expression levels of the universal energy sensor AMPK in Panc1 and Mia-Paca2 we incubated the cells with primary antibodies towards AMPK protein itself, and the active p-AMPK form, since these are as mention, molecule that have significant role in the growth process of tumorigenesis as well.

Table 8.2.3.1 – Data from executed flow cytometry of permeabilizes MIA PaCa cells and Panc-1 29.06.21

	Perm 11.06.2021	GeoMean FITC-A
MIA PaCa-2	Blank	494,6
	2°	78066
	AMPK	7553,4
	p-AMPK	11347,6
Panc -1	Blank	720,2
	2°	2634,8
	Akt	6268,3
	p-Akt	9380,4

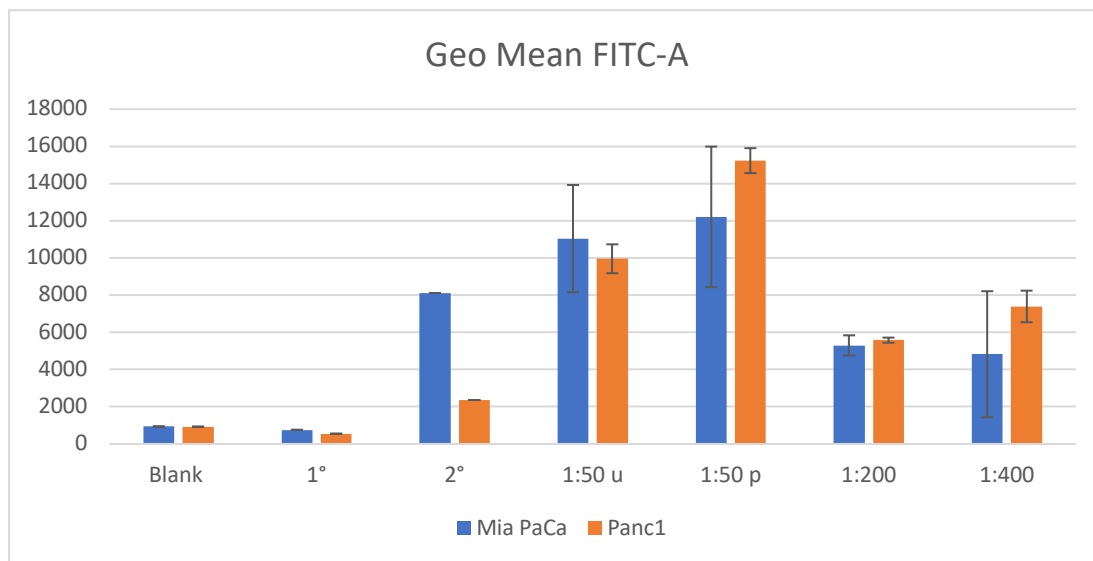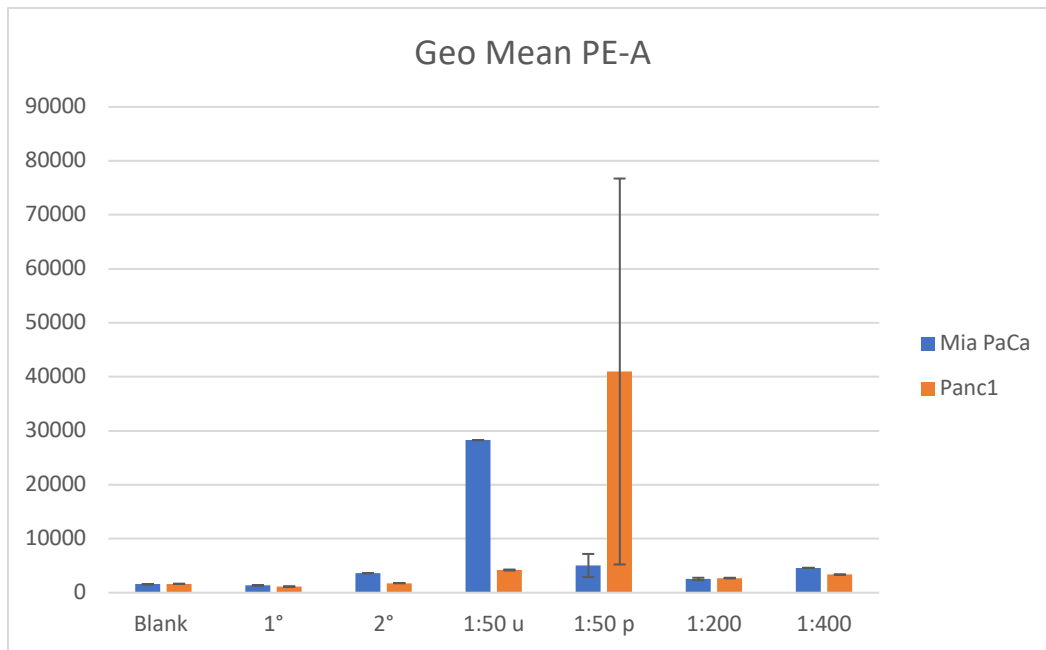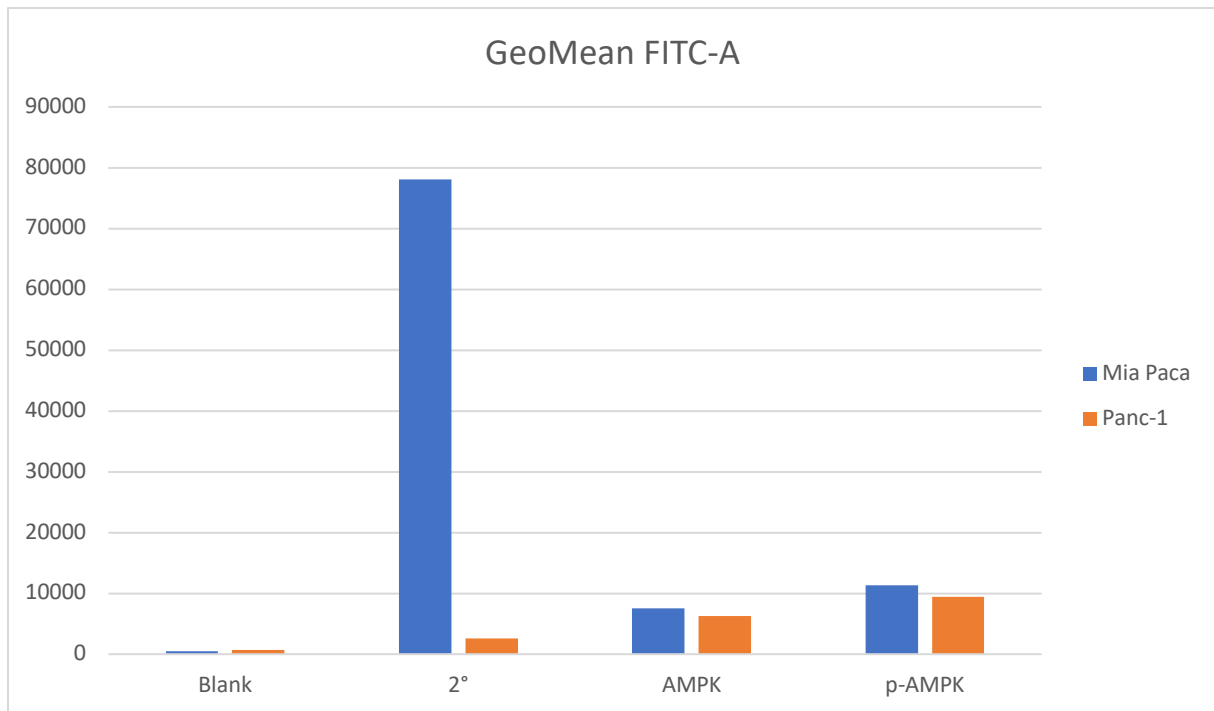*Figure 8.3.3.1 – Bar chart of GeoMean PE-A values presented in Table 1.1 - Data from flow cytometry of permeabilized MIA PaCa cells AMPK and p-AMPK antibodies 29.06.21*
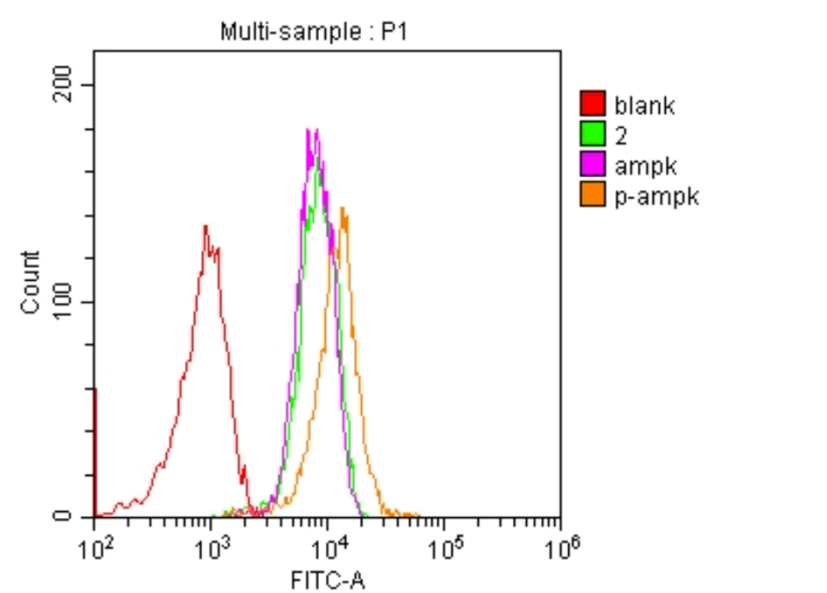
Figure 8.3.3.2 – Overlay histogram for flow cytometry experiment for permeabilized MIA PaCa-2 cells for AMPK and p-AMPK antibodies 29.06.21 with detection of FITC-A channel for gated area (P1)
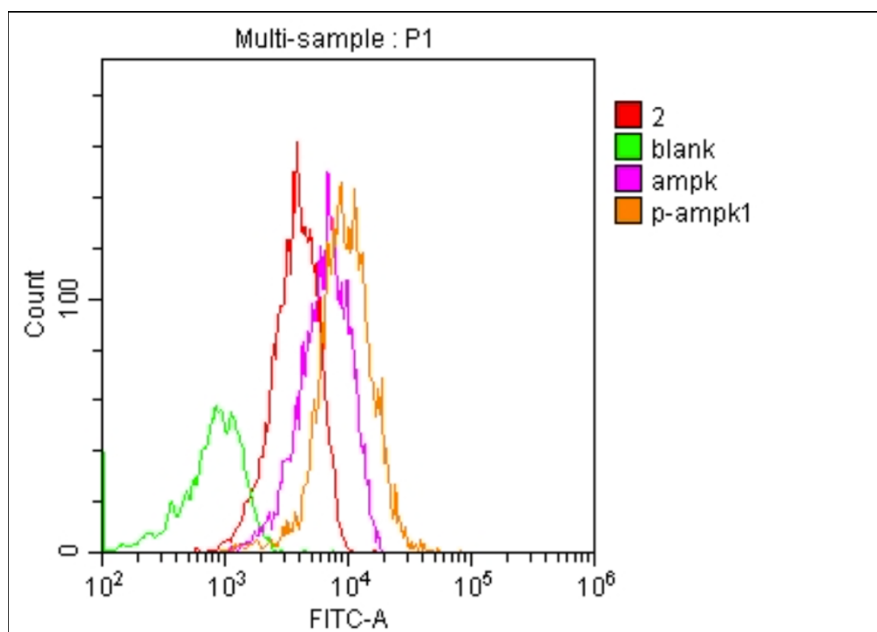
Figure 8.3.3.3 – Overlay histogram for flow cytometry experiment for permeabilized Panc-1 cells 29.06.21 AMPK and p-AMPK antibodies with detection of FITC-A channel for gated area (P1)

Although there was not a clear shift in AMPK expression compared to 2nd antibody control the p- AMPK showed a shift in expression in both cell lines. P-AMKP is shown in several cancer to have a role in cancer growth, progression and prognosis. Phosphorylated AMPK will in neoplastic cells inhibits enzymes of lipogenesis because of increased demand to incorporate fatty acids in the cytoplasmic membrane of proliferating cells(47). Indicating that the expression of p-AMPK is more prominent than AMPK.

8.3.4 Methodological considerations – troubleshooting

To be able to evaluate protein expression using flow cytometry the cell population studies should be representative of viable cells. Challenges with the fixation and permeabilization protocol for both cell lines rendered a cell population with high SSC, indicative of high granularity. To test if fixated cells had intact membranes, the membrane impermeable dye propidium iodine (PI) was used to optimize the fixation technique. PI would stain cells with a disruptive membrane, thus an indicator that the fixation cell process has not been successful. On the other hand, fixated and permeabilized cells should be PI stained as a comparison.

MIA Paca-2
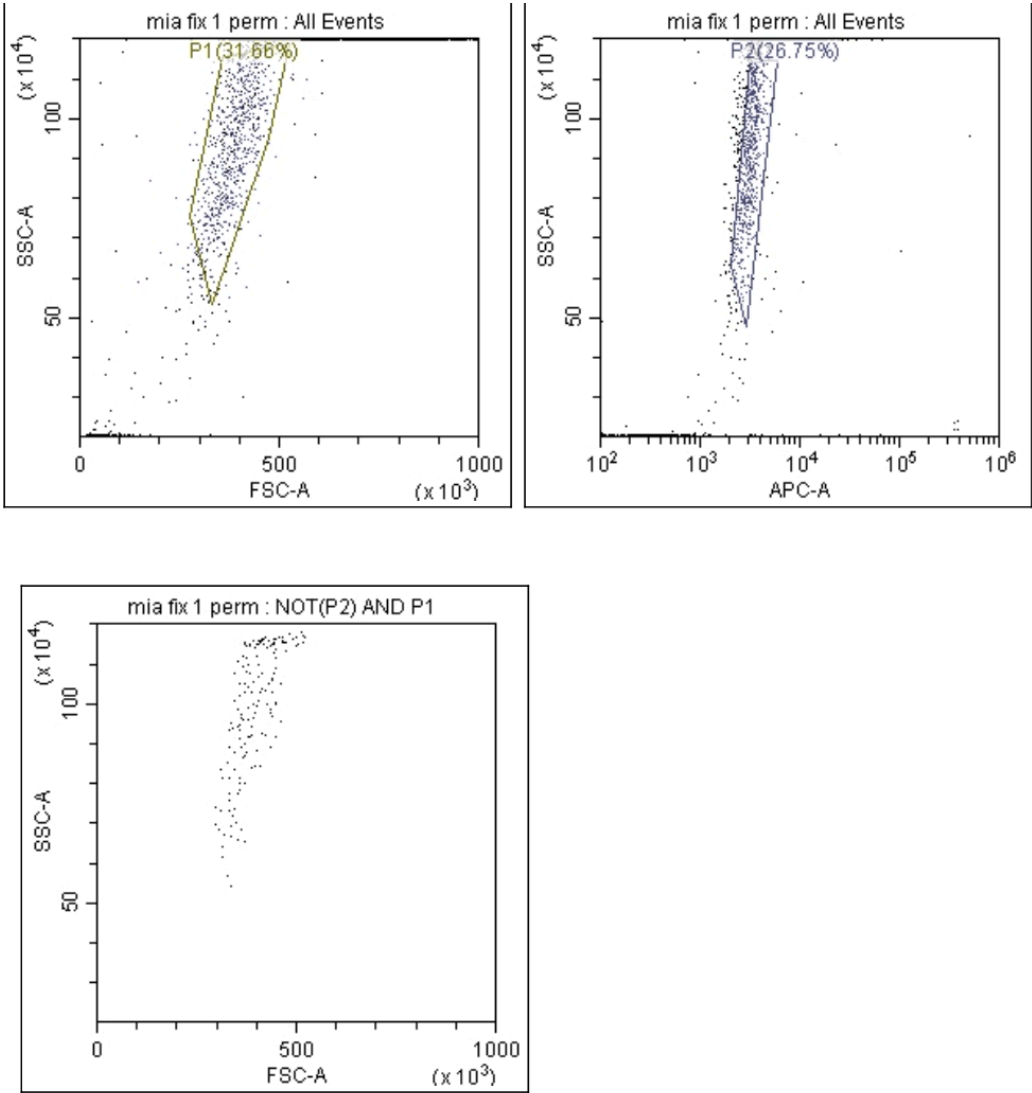
Figure 8.3.4.1– Dot plots from gated MIA PaCa-2 cells with parameter forward scatter (FSC-A and APC-A) for flow cytometry experiment of fixated and permeabilized MIA PaCa cells 19.09.21
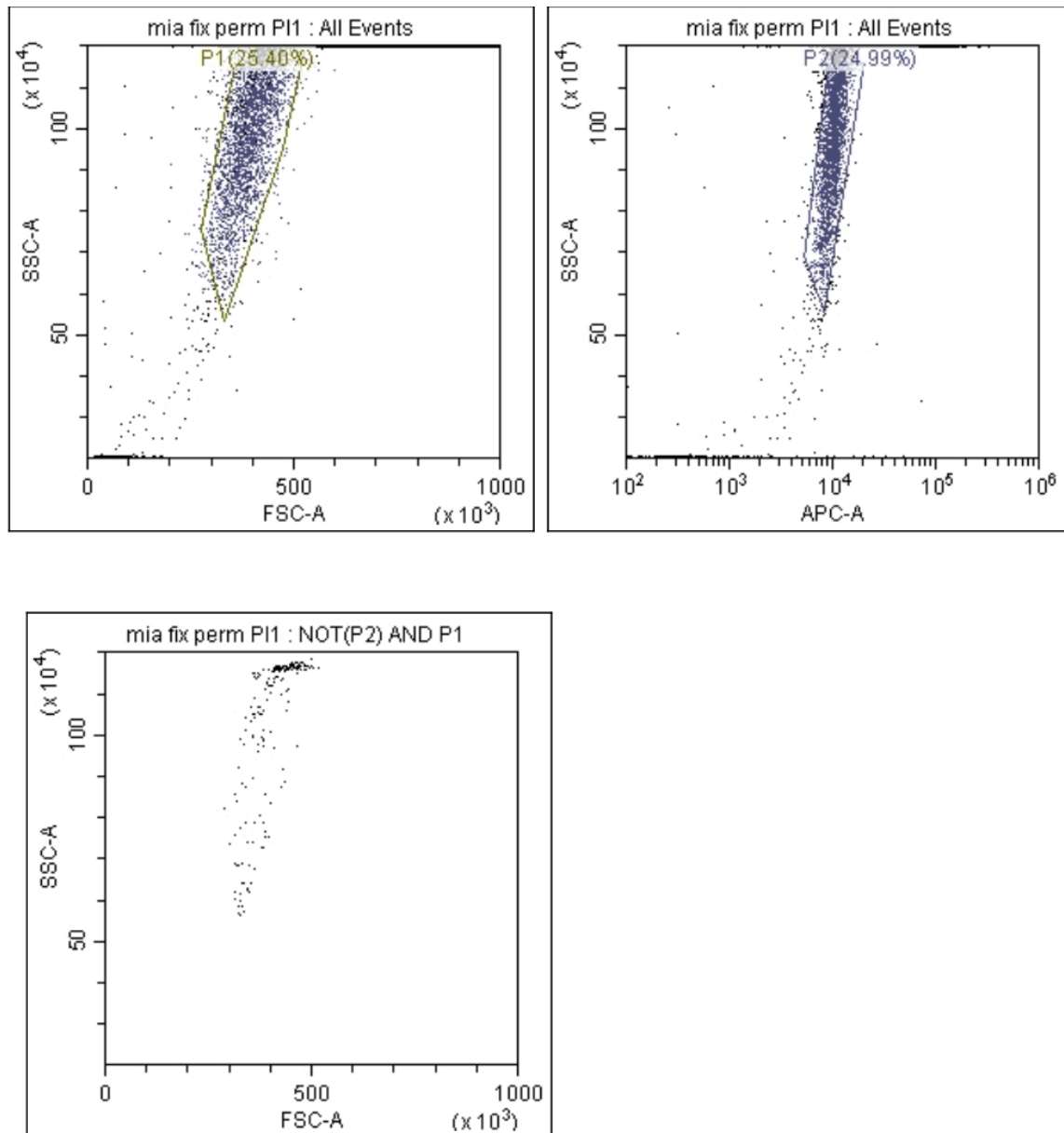
Figure 8.3.4.2 – Dot plots from gated MIA PaCa-2 cells with parameter forward scatter (FSC-A and APC-A) for flow cytometry experiment of fixated and permeabilized MIA PaCa cells with added propidium iodine (PI) 19.09.21

Panc-1
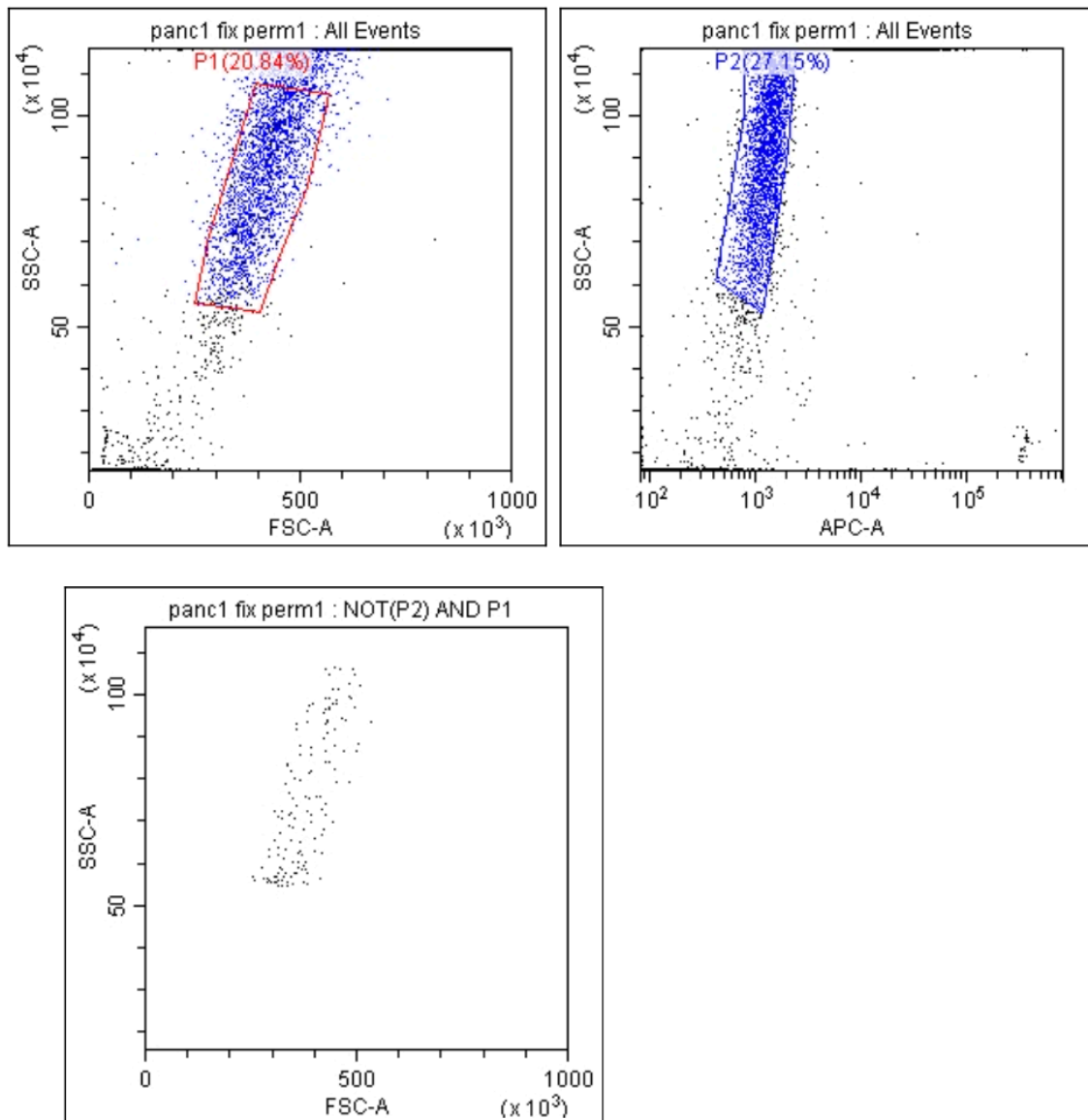
Figure 8.3.4.3 – Dot plots from gated Panc-1 cells with parameter forward scatter (FSC-A and APC-A) for flow cytometry experiment with fixated and permeabilized Panc-1 cells 19.09.21
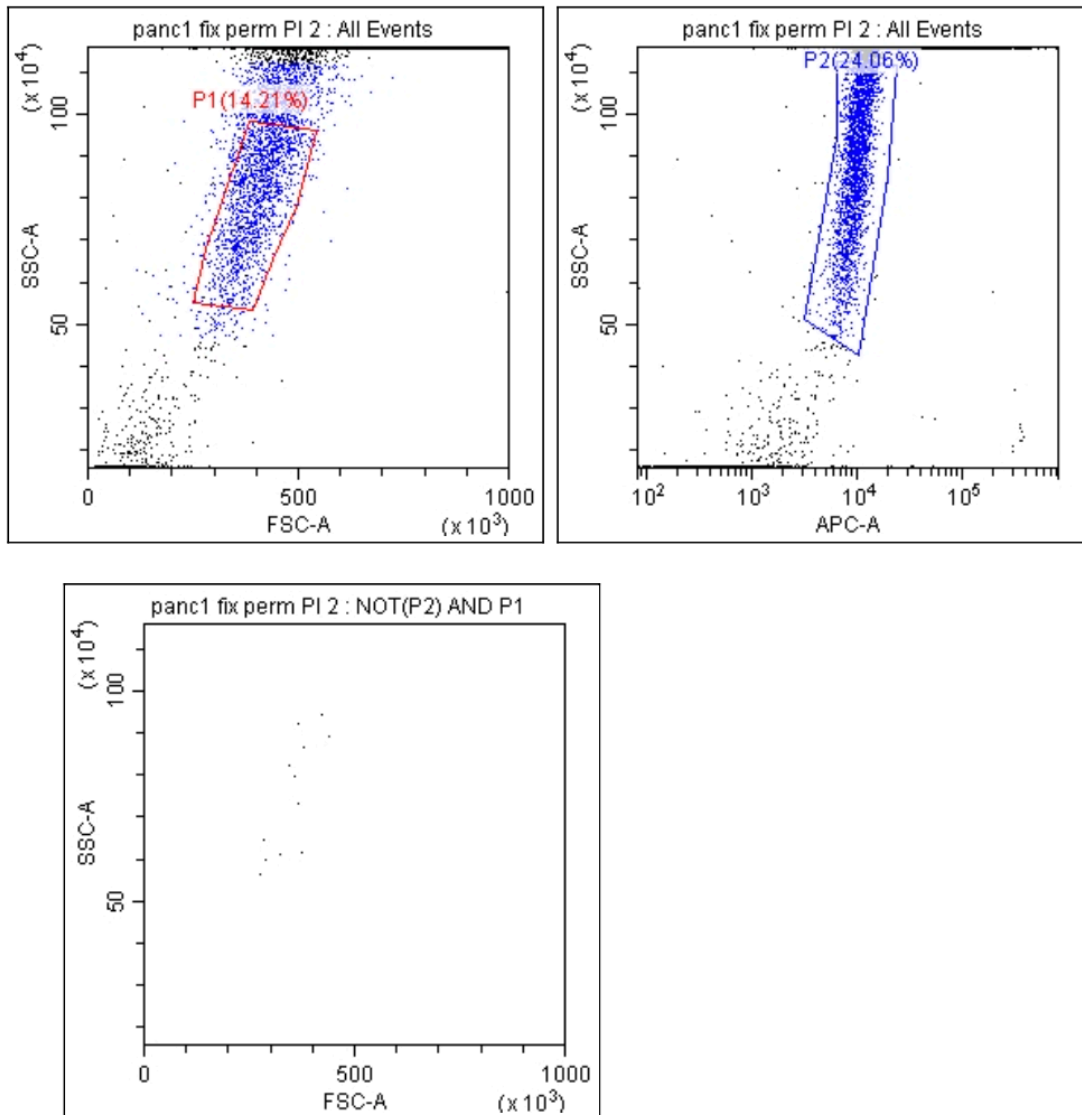
Figure 8.3.4.4 – Dot plots from gated MIA PaCa-2 cells with parameter forward scatter (FSC-A and APC-A) for flow cytometry experiment of fixated and permeabilized Panc-1 cells with added propidium iodine (PI) 19.09.21

All the dot plots for gated cells of fixed and permeabilized MIA PaCa and Panc-1, with and without the addition of PI shows little to no cells. There are few cell populations, and for Panc-1 there is even less. Since there are just a few scattered cells, a run though of MIA PaCa cells were chosen.

MIA PaCa cells were analyzed as the following:

- Fixated
- Fixated with PI
- Permeabilized
- Permeabilized with PI
- Equal mix of fixated and permeabilized cells
- Equal mix of fixated and permeabilized cells with PI

To show an example to obtain the V1L valued the gated dot plots and histogram for fixated MIA PaCa-2 cells are shown in Figure 8.4. (the rest are displayed in appendix). V1L is the ideal gating where gating of cell population in forward scatter FSC-A (P1) and removal of gating of cell population in APC- A channel, where propidium iodine (PI) has its emission.
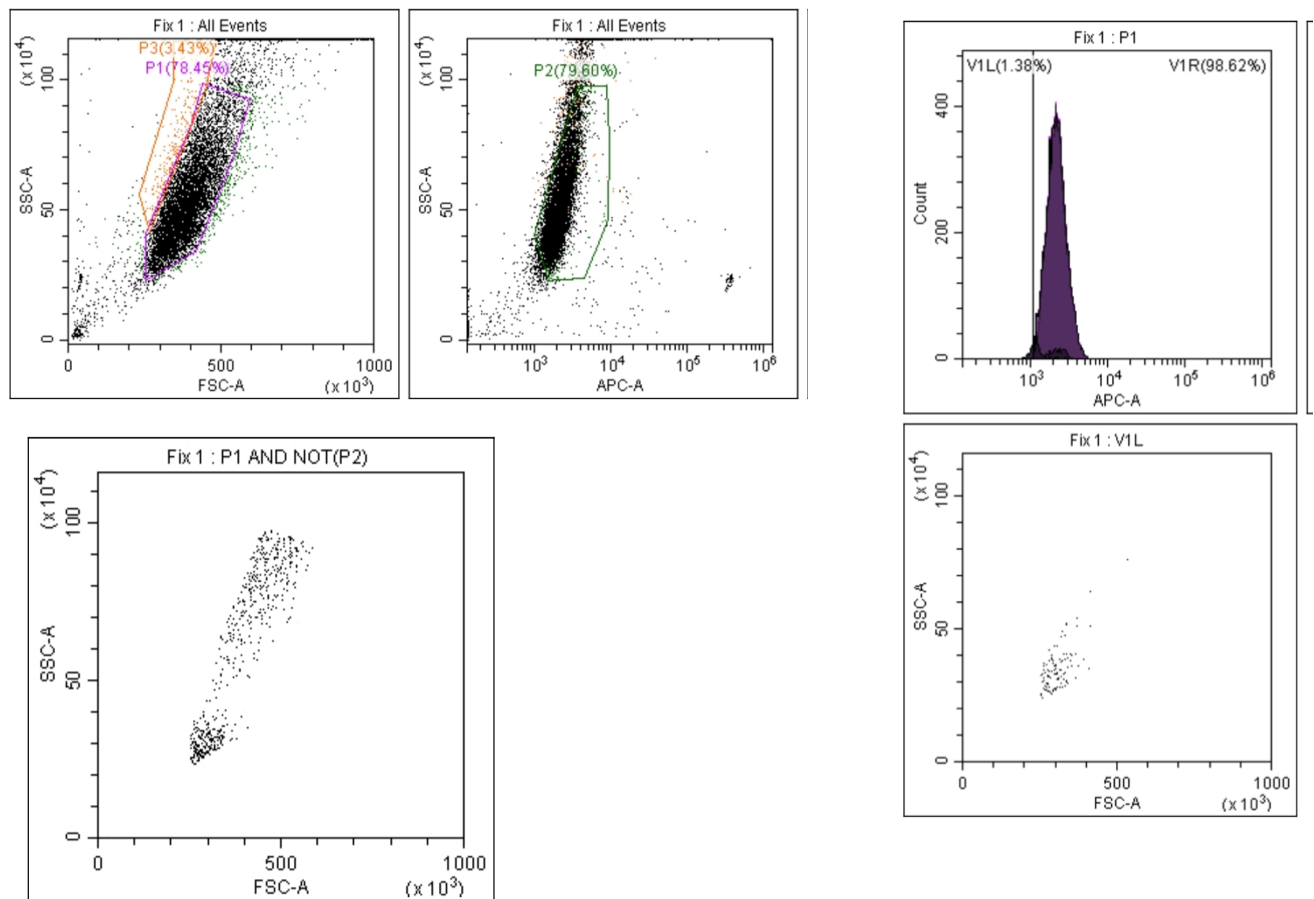
Figure 8.3.4.5 – Schematic overview with dot plots and histogram for optimalization of fixated MIA PaCa-2 cells

The fixated MIA PaCa-2 cells gave a V1L value of 1,38% of the gated cells.

Table 8.3.4.1– V1L values for optimizing the protocol by MIA PaCa-2

	V1L values (%)
Fixated	1,38
Fixated with PI	0,52
Permeabilized	2,83
Permeabilized with PI	0,00
Equal mix of fixated and permeabilized cells	0,73
Equal mix of fixated and permeabilized cells with PI	3,65

9. Discussion

9.1 CCK8

The values obtained from the CCK8 treatment for metformin and phenformin displays differences in cell viability (%) for both cell lines, and as well for rapid and a slower response (6 and 24 hours). As told metformin and phenformin are diabetic type 2 drugs that are been associated with a beneficial effect in cancer patients. (48). Since there are clear values giving higher percentages for cell viability (%) and the values generally give a slight decrease for higher concentrations, it indicates that metformin and phenformin treatment may have effect on pancreatic cancer cell lines. It is also important to note that higher concentrations yield a more gradual decrease in cell viability, rather than the up-and-down values for the lower concentrations. Additionally, cells subjected to phenformin treatment are more reliable.

The execution of CCK8 assays does have sources of error and the values obtained are not enough to conclude the different concentrations that could give results in treatment for pancreatic cancer patients. The metformin treatment at both 6 hours and 24 hours for MIA PaCa-2 are inconclusive and based on only these values the lower concentration of metformin is more effective, which indicates sources of error. Wrongfully calculations when obtaining the correct amount of metformin concentration from the stock solution could have occurred. The CCK8 assays does, however, give a good indicator for which concentrations both for metformin and phenformin are interesting to further examine. When moving forward from the CCK8 assays to analyzing OCT1 expression in treated PANC-1 and MIA PaCa-2 pancreatic cell lines, it was intended to look at three different concentrations. This being the lower, in the middle and highest concentration that yields usable values.

9.2 Flow cytometry

This project was intended to obtain values OCT1 expression for metformin and phenformin treatment of Panc-1 and MIA PaCa-2 cell lines, based on the concentration's values used in the CCK8 assays for both 6 hours rapid response, as well as 24 hours response. After obtained histogram of titrations for OCT1 antibodies and concluding that there were little to no shift that could determine a clear positive expression of OCT1 in both cell lines, the aim shifted to troubleshoot both the protocol and theory before further conducting treatment of metformin and phenformin.

As mentions before, both AKT and AMPK are relevant in the metabolism that contributes to tumorigenesis.(49) Therefore, it was decided to investigate at what expression level Akt and its activated phosphorylated form was detected in both cell lines. High expression of p-AKT is indicative of an active signaling pathway that is a master regulator of glycolysis (50) and cellular growth(51). However, methodological challenges resulted in inconsistency in values, which led us to troubleshoot the initial cell work up before analyzing the cells using flow cytometry.

Immunophenotyping of MIA PaCa-2 and Panc-1 cell lines does reveal differences in morphology and immunohistochemistry. (52). Flow cytometry did clarify that there were two cell populations in MIA PaCa-2 and three in Panc-1, which was confirmed by running non treaded cells from both cell lines only resuspended in PBS trough the flow machine. Since the cell lines did in fact behave and demonstrate the corrected behavior when non-treated, the focus shifted to the fixation and permeabilization step. After optimizing and removing all possible source of error, MIA PaCa-2 was chosen to be examine for its behavior during fixation, permeabilization and if there is a difference occurring from one step to another. By adding PI, which is to stain and would give a clear view if there has been compromised of the cytoplasmic membranes during the permeabilizations process. (53) Ideally, there should have been some higher percentages of V1L values obtained from this, especially the samples containing MIA PaCa-2 cells which is only fixated mixed with equal number of MIA PaCa-2 cells fixated and then permeabilized.

10. Conclusion

Even if there are clear studies that indicate that OCT1 plays a role in the uptake of metformin, and a simple CCK8 dose response assay gives a clear indication that the diabetic drugs implement changes in the pancreatic cancer cell lines MIA PaCa-2 and Panc-1 with there being a decrease in viability, it is to conclude that there are a need to obtain more sensitive and different approach for further use of flow cytometry as an assay for these two particular cell lines.

11. Future work

As mention above in the discussion part, using flow cytometry as an analyzing tool for determine OCT1 expression was not successful, even after attempt to optimize the protocol and therefore may future work be focusing on other biotechnologically tools. q-PCR or RT-PCR is a preferred method. One of the strengths of qPCR is the ability to measure gene expression, which suits with the aim to find OCT1 expression (54). By using a kit to isolate the RNA from both Panc-1 and MIA Pa-Ca-2, such as Direct-zol ᵀᴹ RNA MiniPrep and then cDNA kit for fast cDNA synthesis enabling RT-PCR. By using a 96- well plate, there are opportunities to examine different concentration of both metformin and phenformin treatment, as shown in the CCK8 assays. One of the obstacles for preforming q-PCR was not obtaining a good positive control. Positive control should have a clear expression of OCT1, which healthy liver cells would have expressed. By having the opportunity to obtain liver cells from fish or mammal it would optimize the q-PCR analyzing further.

Another assay is the use of dose response assays with the use of sulforbromophthalein disodium salt which is an organic anion dye used in various studied of membrane carriers expressed in animal tissue and involved in transport of drugs and metabolites and used in vivo studies for assessment for liver functions(55). Both assays would have been greater additions to further expand the OCT1 expression executed in pancreatic cancer cell lines with the treatment of metformin and phenformin by giving corrections or additions to the response found during the CCK8 assays. Better optimizing of flow cytometry protocol and then being

able to look into the changes occurring after treatment of metformin and phenformin, with the values found in the CCK8 would have been the most ideal for this project.

12. Literature list

1.   Pancreatic Cancer Treatment (Adult) (PDQR) - Patient Version
https://www.cancer.gov/types/pancreatic/patient/pancreatic-treatment-pdq#section/all
National Cancer Institue at the National Institutes of health [updated 11.12.2020

2.   Jiao L, Li D. Epidemiology and Prospects for Prevention of Pancreatic Cancer. Pancreatic Cancer. New York, NY: Springer New York; 2010. p. 3-25.

3.   Research WCRFAIfC. Food, Nutrition, Physical Activity, and the Prevention of Cancer: a Global Perspective. Washington DC: AICR; 2007.

4.   Greer JB, Whitcomb DC, Brand RE. Genetic predisposition to pancreatic cancer: a brief review. Am J Gastroenterol. 2007;102(11):2564-9.

5.   Barnes JL, Zubair M, John K, Poirier MC, Martin FL. Carcinogens and DNA damage. Biochemical Society Transactions. 2018;46(5):1213-24.

6.   Prevention CfDCa. Obesity and Cancer Division of Cancer Prevention and Control, Centers for Disease Control and Prevention 2021 [Available from:
https://www.cdc.gov/cancer/obesity/index.htm.

7.   Sato K, Hikita H, Myojin Y, Fukumoto K, Murai K, Sakane S, et al. Hyperglycemia enhances pancreatic cancer progression accompanied by elevations in phosphorylated STAT3 and Myc levels. Plos one. 2020;15(7):e0235573.

8.   Søreide K, Stättner S. Textbook of Pancreatic Cancer: Principles and Practice of Surgical Oncology: Springer Nature; 2021.

9.   Deer EL, González-Hernández J, Coursen JD, Shea JE, Ngatia J, Scaife CL, et al. Phenotype and genotype of pancreatic cancer cell lines. Pancreas. 2010;39(4):425-35.

10.   Stolzenberg-Solomon RZ, Graubard BI, Chari S, Limburg P, Taylor PR, Virtamo J, et al. Insulin, glucose, insulin resistance, and pancreatic cancer in male smokers. Jama. 2005;294(22):2872-8.

11.   Pisani P. Hyper-insulinaemia and cancer, meta-analyses of epidemiological studies. Archives of physiology and biochemistry. 2008;114(1):63-70.

12.   Michaud DS, Wolpin B, Giovannucci E, Liu S, Cochrane B, Manson JE, et al. Prediagnostic plasma C-peptide and pancreatic cancer risk in men and women. Cancer Epidemiology and Prevention Biomarkers. 2007;16(10):2101-9.

13.   Stattin P, Björ O, Ferrari P, Lukanova A, Lenner P, Lindahl B, et al. Prospective Study of Hyperglycemia and Cancer Risk. Diabetes Care. 2007;30(3):561-7.

14.   Gapstur SM, Gann PH, Lowe W, Liu K, Colangelo L, Dyer A. Abnormal glucose metabolism and pancreatic cancer mortality. Jama. 2000;283(19):2552-8.

15.   Batty GD, Shipley MJ, Marmot M, Smith GD. Diabetes status and post-load plasma glucose concentration in relation to site-specific cancer mortality: findings from the original Whitehall study. Cancer Causes & Control. 2004;15(9):873-81.

16.   Offord E. Markers of oxidative damage and antioxidant protection: current status and relevance to disease. Free Radic Res. 2000;33:S5-S19.

17.   Grimm D, Lieb J, Weyer V, Vollmar J, Darstein F, Lautem A, et al. Organic Cation Transporter 1 (OCT1) mRNA expression in hepatocellular carcinoma as a biomarker for sorafenib treatment. BMC cancer. 2016;16(1):1-8.

18.   Koepsell H, Lips K, Volk C. Polyspecific organic cation transporters: structure, function, physiological roles, and biopharmaceutical implications. Pharmaceutical research. 2007;24(7):1227-51.

19.   Lozano E, Herraez E, Briz O, Robledo VS, Hernandez-Iglesias J, Gonzalez-Hernandez A, et al. Role of the plasma membrane transporter of organic cations OCT1 and its genetic variants in modern liver pharmacology. BioMed research international. 2013;2013.

20.   Schorn S, Dicke A-K, Neugebauer U, Schröter R, Friedrich M, Reuter S, et al. Expression and Function of Organic Cation Transporter 2 in Pancreas. Frontiers in Cell and Developmental Biology. 2021;9(1328).

21.   Motohashi H, Inui K-i. Pharmacological and toxicological significance of the organic cation transporters OCT and MATE: Drug disposition, interaction and toxicity. Organic cation transporters: Springer; 2016. p. 73-92.

22.   Annibaldi A, Widmann C. Glucose metabolism in cancer cells. Current Opinion in Clinical Nutrition & Metabolic Care. 2010;13(4):466-70.

23.   Hamanaka RB, Chandel NS. Targeting glucose metabolism for cancer therapy. Journal of Experimental Medicine. 2012;209(2):211-5.

24.   Shaw RJ. Glucose metabolism and cancer. Current opinion in cell biology. 2006;18(6):598-608.

25.   Pouysségur J, Dayan F, Mazure NM. Hypoxia signalling in cancer and approaches to enforce tumour regression. Nature. 2006;441(7092):437-43.

26.   Robey RB, Hay N, editors. Is Akt the "Warburg kinase"?—Akt-energy metabolism interactions and oncogenesis. Seminars in cancer biology; 2009: Elsevier.

27.   Nagel J. Exploring the role of chemotherapy-induced anastasis in triple-negative breast cancer: University of British Columbia; 2019.

28.   Herzig S, Shaw RJ. AMPK: guardian of metabolism and mitochondrial homeostasis. Nature reviews Molecular cell biology. 2018;19(2):121-35.

29.   Vara-Ciruelos D, Russell FM, Hardie DG. The strange case of AMPK and cancer: Dr Jekyll or Mr Hyde? Open biology. 2019;9(7):190099.

30.   Owen MR, Doran E, Halestrap AP. Evidence that metformin exerts its anti-diabetic effects through inhibition of complex 1 of the mitochondrial respiratory chain. Biochemical journal. 2000;348(3):607-14.

31.   Kasznicki J, Sliwinska A, Drzewoski J. Metformin in cancer prevention and therapy. Annals of translational medicine. 2014;2(6).

32.   Smith U, Gale E. Cancer and diabetes: are we ready for prime time? Diabetologia. 2010;53(8):1541-4.

33.   Evans J. Donnelly lA, Emslie-Smith AM, Alessi DR, Morris AD. Metformin and reduced risk of cancer in diabetic patients. Brit Med J. 2005;330(7503):1304-5.

34.   de la Cruz López KG, Toledo Guzmán ME, Sánchez EO, García Carrancá A. mTORC1 as a regulator of mitochondrial functions and a therapeutic target in cancer. Frontiers in oncology. 2019;9:1373.

35.   Chiang GG, Abraham RT. Targeting the mTOR signaling network in cancer. Trends in molecular medicine. 2007;13(10):433-42.

36.   Cairns S, Shalet S, Marshall A, Hartog M. A comparison of phenformin and metformin in the treatment of maturity onset diabetes. Diabete & metabolisme. 1977;3(3):183-8.

37.   García Rubiño M, Carrillo E, Ruiz Alcalá G, Domínguez-Martín A, A Marchal J, Boulaiz H. Phenformin as an anticancer agent: challenges and prospects. International journal of molecular sciences. 2019;20(13):3316.

38.   Millipore E. MuseTM Count & Viabilty kit User´s guide Millipore, EMD 2013.

39.   Millipore E. Precise and Accurate Counts and Viability Measurements Across Multiple Cell Lines Using the Muse™ Cell Count & Viability Assay. BioTechniques. 2012;52(3):200-3.

40.	Rampersad SN. Multiple applications of Alamar Blue as an indicator of metabolic function and cellular health in cell viability bioassays. Sensors. 2012;12(9):12347-60.

41.	Page B, PAGE M, NOEL C. A new fluorometric assay for cytotoxicity measurements in-vitro. International journal of oncology. 1993;3(3):473-6.

42.	GBiosciences. AlamarBlue Cell Viability Assay Reagent G-Biosciences 2016.

43.	Rahman M. Introduction to flow cytometry. AbD serotec. 2006:1-33.

44.	Technology CS. Flow Cytometry, Methanol Permeabilization Protocol Cell Signaling Technology Cell Signaling Technology 2019 [Available from: https://www.rndsystems.com/resources/protocols/flow-cytometry-protocol-analysis-cell-viability-using-propidium-iodide

45.	Riccardi C, Nicoletti I. Analysis of apoptosis by propidium iodide staining and flow cytometry. Nature protocols. 2006;1(3):1458-61.

46.	systems RD. Propidioum Iodine Cell Viabilty Flow Cytometry Protocol R6D Systems [Available from: https://www.rndsystems.com/resources/protocols/flow-cytometry-protocol-analysis-cell-viability-using-propidium-iodide

47.	Khabaz MN, Abdelrahman AS, Al-Maghrabi JA. Expression of p-AMPK in colorectal cancer revealed substantial diverse survival patterns. Pakistan journal of medical sciences. 2019;35(3):685.

48.	Heckman-Stoddard BM, Gandini S, Puntoni M, Dunn BK, DeCensi A, Szabo E, editors. Repurposing old drugs to chemoprevention: the case of metformin. Seminars in oncology; 2016: Elsevier.

49.	Han F, Li C-F, Cai Z, Zhang X, Jin G, Zhang W-N, et al. The critical role of AMPK in driving Akt activation under stress, tumorigenesis and drug resistance. Nature communications. 2018;9(1):1-16.

50.	Huang S-W, Kao J-K, Wu C-Y, Wang S-T, Lee H-C, Liang S-M, et al. Targeting aerobic glycolysis and HIF-1α expression enhance imiquimod-induced apoptosis in cancer cells. Oncotarget. 2014;5(5):1363.

51.	Wang K, Cao F, Fang W, Hu Y, Chen Y, Ding H, et al. Activation of SNAT1/SLC38A1 in human breast cancer: correlation with p-Akt overexpression. BMC cancer. 2013;13(1):1-9.

52.	Gradiz R, Silva HC, Carvalho L, Botelho MF, Mota-Pinto A. MIA PaCa-2 and PANC-1–pancreas ductal adenocarcinoma cell lines with neuroendocrine differentiation and somatostatin receptors. Scientific reports. 2016;6(1):1-14.

53.   Juan WS, Lin HW, Chen YH, Chen HY, Hung YC, Tai SH, et al. Optimal Percoll concentration facilitates flow cytometric analysis for annexin V/propidium iodine-stained ischemic brain tissues. Cytometry Part A. 2012;81(5):400-8.

54.   Scientific T. What is qPCR? ThermoFisher Scientific 2020 [Available from: https://www.thermofisher.com/blog/ask-a-scientist/what-is-qpcr/.

55.   MedChemExpress. Sulfobromophthalein disodium salt [Available from: https://www.medchemexpress.com/sulfobromophthalein-disodium-salt.html.

Appendix

1.AlamarBlue assay:

Settings Information
- TUNE (s/n 2063)
  - Lm1   540, 590
  - Fluorescence
  - Endpoint
- More Settings
  - ReadOrder Row
  - Show Optimizer On
- PMT and Optics
  - Integration Time 140 ms
  - Read from Bottom
  - Read Height 1.00 mm

Plate2

	1	2	3	4	5	6	7	8	9	10	11	12
A	5.0e6	6.2e6	7.7e6	7.6e6	7.8e6	6.2e6	7.0e6	1.4e7	1.8e7	2.3e7	4.3e7	3.1e7
B	5.4e6	5.8e6	7.0e6	7.3e6	8.3e6	5.9e6	6.8e6	1.6e7	2.0e7	2.1e7	4.4e7	3.3e7
C	5.6e6	5.9e6	7.3e6	8.1e6	9.2e6	5.8e6	6.3e6	1.3e7	1.9e7	2.1e7	4.1e7	3.2e7
D	5.4e6	6.1e6	6.6e6	7.1e6	8.6e6	6.1e6	1.2e7	1.4e7	1.8e7	2.0e7	4.4e7	3.6e7
E	5.4e6	6.3e6	6.9e6	8.0e6	8.0e6	6.0e6	6.0e6	1.4e7	2.0e7	2.1e7	4.3e7	3.3e7
F	5.0e6	6.1e6	7.0e6	7.0e6	8.5e6	5.9e6	7.5e6	1.4e7	1.9e7	2.1e7	4.3e7	3.4e7
G	4.8e6	4380.0	5293.0	5076.0	4607.0	5657.0	3.8e7	4.1e7	4.2e7	4.6e7	4.1e7	4.3e7
H	5736.0	4383.0	5330.0	5247.0	4379.0	5384.0	5065.0	5019.0	4746.0	4563.0	4970.0	5386.0

Reduction Settings
Wavelength Combination : !Lm1

Read Information
SpectraMax Paradigm
ROM vV1.2 b100 29.09.2014
Start Read : 2:18 PM 3/3/2021
Mean Temperature : 24 °C

Figure 1.1 – Values of AlamarBlue assay of Panc- 1 and MIA PaCa cell line – read using SpectraMax Paradigm Microplate Reader 3.3.2021

The plate outline is:
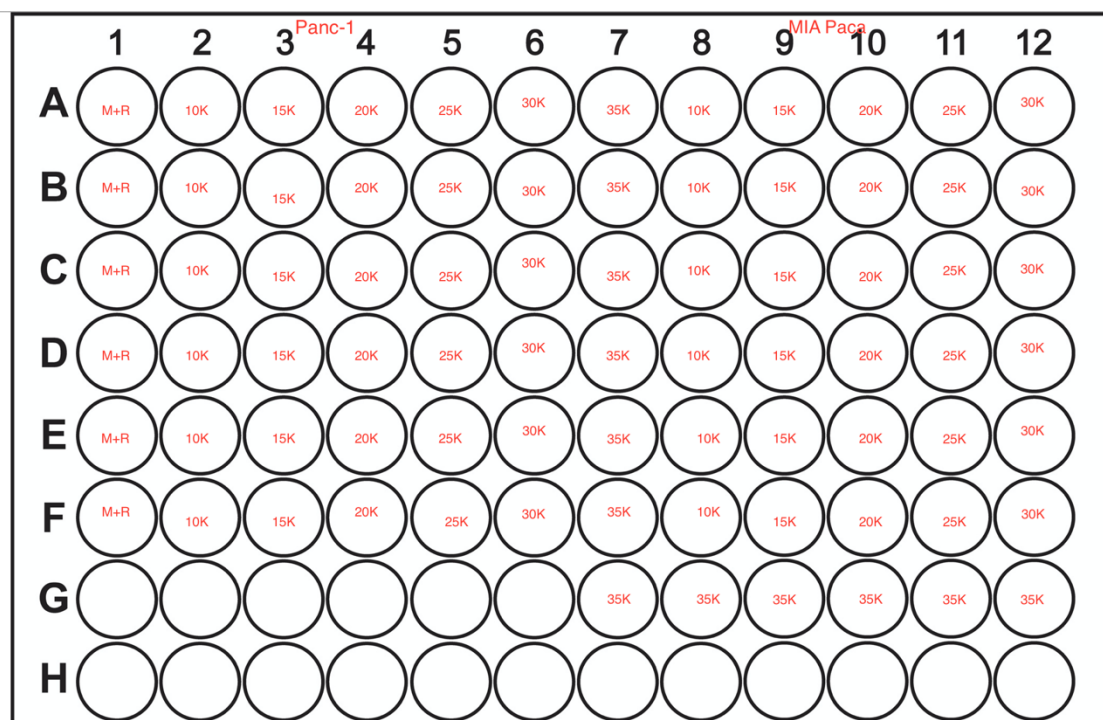
***Figure 1.2 – Plate outline for Plate values of AlamarBlue assay of Panc- 1 and MIA PaCa cell line** 3.3.2021*

Notations: M+R – medium with added 10% Resazurin, 10K - Cellsuspension with 10 000 cell density with 10% added Resazurin

Plate1

	1	2	3	4	5	6	7	8	9	10	11	12
A	3.3e8	2.2e4	2.2e4	2.0e4	2.2e4	2.1e4	2.0e4	2.3e4	2.1e4	2.3e4	2.2e4	3.3e8
B	2.3e7	4.5e7	7.9e7	7.8e7	5.3e7	7.1e7	9.3e7	1.9e8	7.0e7	1.3e8	1.3e8	1.9e8
C	2.3e7	4.7e7	8.2e7	7.5e7	5.6e7	6.8e7	1.0e8	2.0e8	7.2e7	1.3e8	1.5e8	1.9e8
D	2.4e7	4.5e7	5.1e7	7.3e7	5.3e7	6.0e7	6.7e7	2.0e8	7.6e7	1.2e8	1.3e8	1.8e8
E	2.4e7	3.3e7	5.2e7	4.8e7	8.0e7	6.6e7	6.8e7	1.9e8	7.8e7	1.1e8	1.3e8	1.1e8
F	2.4e7	4.1e7	5.9e7	4.9e7	7.7e7	6.6e7	7.1e7	2.0e8	7.4e7	1.2e8	1.6e8	1.2e8
G	1.6e5	3.2e4	2.0e4	4.5e4	4.5e4	2.4e4	3.9e4	2.2e8	1.8e8	1.5e8	1.6e8	1.7e8
H	3.5e8	2.2e4	2.0e4	2.0e4	2.4e4	2.0e4	2.0e4	2.1e4	2.3e4	2.4e4	2.3e4	3.4e8

Settings Information
TUNE (s/n 2063)
Lm1   540, 590
Fluorescence
Endpoint
More Settings
ReadOrder Row
Show Optimizer On
PMT and Optics
Integration Time 140 ms
Read from Bottom
Read Height 3.36 mm

Read Information
SpectraMax Paradigm
ROM vV1.2 b100 29.09.2014
Start Read : 5:21 PM 3/5/2021
Mean Temperature : 24 °C

Reduction Settings
Wavelength Combination : !Lm1

Figure 1.3 Values of AlamarBlue assay of Panc- 1 and MIA PaCa cell line *–   read using*
SpectraMax Paradigm Microplate Reader 5.3.2021

The plate outline is
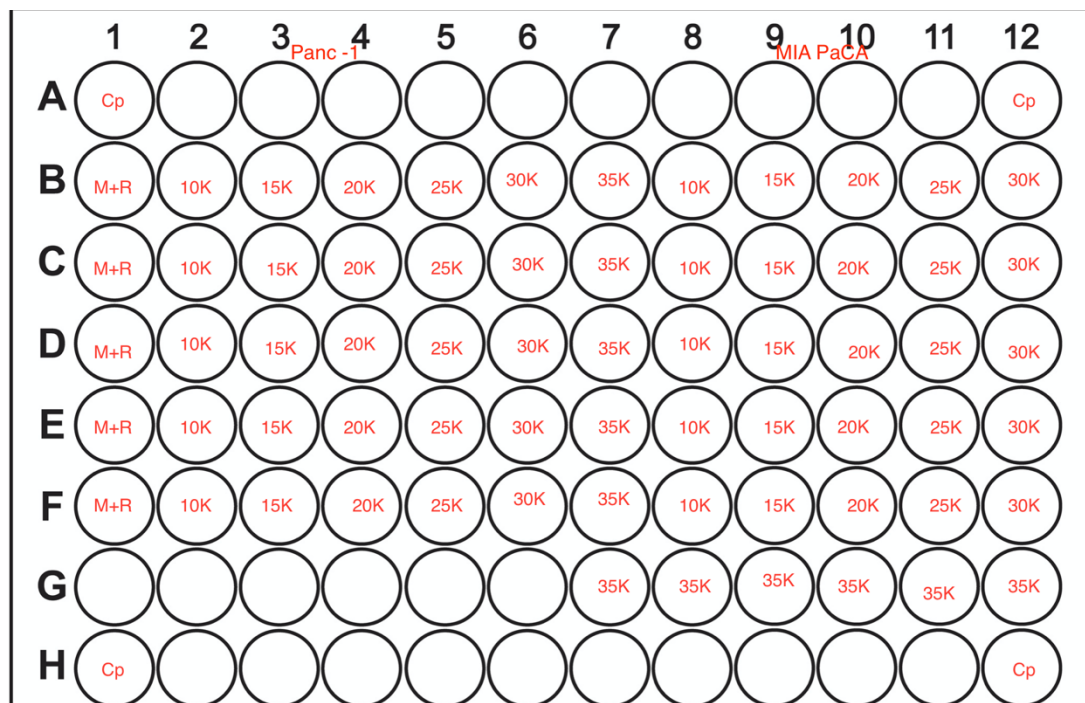
Figure 1.4 – Plate outline for Plate values of AlamarBlue assay of Panc- 1 and MIA PaCa
cell line **5.3.2021**

Notations: Cp – Positive control – Resorufin, *M+R – medium with added 10% Resazurin,*

10K - Cellsuspension with 100 000 cell density with 10% added Resazurin

Table 1.1 - Panc – 1 Read and average values from both plates with cell density from 10-
35 K

Plate 3.3.21	10K	15K	20K	25K	30K	35 K
	6188132	7737524	7563327	7790302	6218624	7028713
	5825342	7032975	7339160	8330232	5893620	6753122
	5906584	7268070	8069348	9224599	5825938	6275000
	6111162	6559857	7111498	8566249	6058254	12386652
	6339198	6925602	7991580	8014194	6000166	5963392
	6141480	6961364	7033386	8526429	5924002	7461056

Average value	6085316,333	7080898,667	7518049,83	8408667,5	5986767,333	6879472,75
Plate 5.3.21	44853572	78858056	77784032	53321916	71112280	93480544
	47408520	81833536	74699040	56462744	68188872	103487240
	44948540	50775808	72977776	52954860	60428784	66807920
	32640996	51676820	47937628	79814592	65626280	68101968
	40501668	59466420	49191144	76654544	66166752	71186480
	44853572	78858056	77784032	53321916	71112280	93480544
Average value	44513174,4	79849882,67	75811220	62088428,67	67105874,67	82757449,33

Table 1.2 – MIA PaCa Read and average values from both plates with cell density from 10-35 K

Plate 3.3.21	10K	15K	20K	25K	30K	35 K
	13578322	17599744	22725908	42536048	30745924	38343828
	15853440	19671086	21263764	43632160	33082422	40571876
	13354810	19426438	21145632	40703760	32024354	41730612
	14286734	18277770	20284940	44123828	35626892	45846596
	14455985	19846200	20947542	43430788	33339154	40775624
	14082203	18540364	21278668	42669836	34092004	43273760
Average value	14268582,33	18893600,33	21274409	42849403,33	33151791,67	41757049,33
Plate 5.3.21	189321920	70014720	128990056	133489216	187673888	215350640
	195554080	72159768	134477216	145077760	185968224	177545776
	204279728	76062768	120887856	134967088	178052000	147937520
	192110048	78474896	114141872	126578864	107893744	163352368
	198270176	73695816	115783136	158981232	121998088	169406320
Average value	195907190,4	74081593,6	122856027	139818832	156317188,8	174718524,8

2. CCK8

Table 2.1 – Cell viability (%) for PANC-1 Metformin 24 hours

Concentration	Average	Cell viability (%)	Std
100	0,95242	116,7873127	0,338075254
250	0,64745	79,39138787	0,459604194
500	1,218116667	149,3674767	0,39332336
1000	0,919916667	112,8017004	0,419659702
2000	1,204283333	147,6712105	0,453298522
4000	0,9285	113,8591077	0,522697358
8000	1,212	148,6174409	0,535252673

Table 2.2 – Cell viability (%) for PANC-1 Metformin 6 hours

Concentration	Average	Cell viability (%)	Std
100	0,733866667	88,89965677	0,053649821
250	0,8646	104,7365233	0,151346093
500	0,850233333	102,9961639	0,110198745
1000	1,0679	129,3640218	0,348021206
2000	0,876766667	106,2103775	0,08814178
4000	0,9285	112,482132	0,143265244
8000	0,799813333	96,88835049	0,114785263

Table 2.3 – Cell viability (%) for PANC-1 Phenformin 24 hours

Concentration	Average	Cell Viability (%)	Std
25	1,337366667	119,612432	0,146858106
50	0,950466667	85,00857122	0,144541906
100	0,96585	86,38443765	0,414398729
250	0,728666667	65,17105165	0,13997685
500	0,67598	60,4588209	0,295985586
1000	0,90215	80,6871879	0,449685354
2000	0,63656	56,93314452	0,175020082

Table 2.4 – Cell viability (%) for PANC-1 Phenformin 6 hours

Concentration	Average	Cell viability (%)	Std
25	0,8101	85,14521949	0,306341835
50	0,6888	72,39603405	0,235793957
100	0,819733333	86,15772694	0,122555797
250	0,773733333	81,3229163	0,052793592
500	0,9567	100,5535508	0,383733462
1000	1,2753	134,0398697	0,299801334
2000	0,672	70,63027713	0,305084529

Table 2.5 – Cell viability (%) for MIA PaCa Metformin 24 hours

Concentration	Average	Cell viability (%)	Std
100	1,959933333	102,5042929	0,673536504
250	1,089916667	57,00251911	0,821333003
500	1,404638333	73,46242689	0,83728361
1000	1,4219	74,36521011	0,966788562
2000	1,84242	96,35835883	0,971880796
4000	1,9999	104,5934991	0,837100488
8000	2,542966667	132,9968707	0,551851964

Table 2.6 – Cell viability (%) for MIA PaCa Metformin 6 hours

Concentration	Average	Cell viability (%)	Std
100	0,5804	73,17811213	0,030764753
250	0,703266667	88,66941246	0,304282785
500	0,7627	96,16289821	0,134053385
1000	0,7623	96,11246533	0,007937254
2000	1,134433333	143,0318568	0,113521643
4000	1,0525	132,6973187	0,060898467
8000	0,821233333	103,54291	0,060852718

Table 2.7 – Cell viability (%) for MIA PaCa Phenformin 24 hours

Concentration	Average	Cell Viability (%)	Std
25	1,931433333	97,5824583	0,396259373
50	1,351766667	68,29576362	0,713891159
100	1,378316667	69,63715823	0,566804013
250	1,6267	82,18631323	0,848200337
500	2,2906	115,728757	0,415124656
1000	1,916483333	96,8271344	0,66553046
2000	1,38685	70,06829071	0,913611453

Table 2.8 – Cell viability (%) for MIA PaCa Phenformin 6 hours

Concentration	Average	Cell viability (%)	Std
25	0,494933333	64,58179288	0,110850906
50	0,580333333	75,72528381	0,026385097
100	0,5833	76,11239181	0,118069005
250	0,709866667	92,62754991	0,121963533
500	0,777333333	101,4309947	0,121963533
1000	0,6529	85,19420643	0,011873079
2000	0,5601	73,08512026	0,057506261

Table 2.8 - Raw values given from read using SpectraMax Paradigm Microplate Reader 26.3.2021 – Plate 1 24 hours

	1	2	3	4	5	6	7	8	9	10	11	12
A	0.5312	0.5507	0.6259	0.5476	0.5607	0.6438	2.3043	2.4029	2.1594	2.3393	2.2563	2.7584
B	0.6597	0.8803	0.9142	0.4642	0.4228	0.6066	3.3899	2.8151	2.8227	0.592	0.5932	0.6242
C	0.4391	0.7679	0.1861	0.7129	0.575	0.6792	2.6757	2.2203	1.7309	0.9758	2.146	1.4062
D	0.5654	1.3323	1.4367	0.9845	0.7173	0.1848	2.6309	2.291	2.7068	2.1059	2.5332	1.7299
E	0.6132	0.788	0.7507	0.6533	0.9078	0.5588	2.5742	2.5493	1.6143	0.2124	2.699	2.1227
F	1.4273	0.7358	1.5637	0.6436	1.7679	1.0044	1.8551	2.3704	2.2333	1.437	2.1363	1.9368
G	0.8697	1	1.2756	0.8273	1.1984	0.9219	1.9739	1.6724	1.8563	1.6357	2.048	2.2431
H	0.6469	0.38	0.6598	0.4809	0.7866	0.1617	1.9698	2.135	1.5967	1.7127	2.1702	2.4543

Table 2.9 - Raw values given from read using SpectraMax Paradigm Microplate Reader 9.4.2021 – Plate 1 24 hours

	1	2	3	4	5	6	7	8	9	10	11	12
A	0.286	1.4452	1.4524	2.4305	1.145	1.3809	1.2378	1.8898	1.4781	1.937	1.1824	1.4023
B	1.8447	1.9211	1.052	0.8105	0.8787	1.2821	2.0648	2.1007	2.0614	2.5091	2.3998	1.6018
C	1.6308	1.1734	0.6315	0.7604	1.6758	1.0096	1.7815	0.2124	1.591	2.7792	2.4184	1.7733
D	1.6865	1.4868	0.718	0.7128	0.7805	1.9666	0.7844	0.799	0.1795	2.9369	2.3335	2.1042
E	0.9998	1.7292	0.6386	0.7748	0.6182	0.8591	0.6145	0.5945	0.5846	1.5297	1.9065	1.2899
F	0.8577	1.0409	1.6833	0.7777	0.7529	0.8097	0.6126	0.6862	0.6702	1.0283	0.6807	1.0508
G	0.2038	0.2302	0.3054	1.0167	0.8006	0.9379	0.3089	0.3418	0.3862	0.6654	0.6726	0.8458
H	1.1523	1.1417	1.1614	1.1946	1.3295	1.488	2.5666	2.926	1.5661	1.8562	1.3156	2.0796

Table 2.10 - Raw values given from read using SpectraMax Paradigm Microplate Reader 26.3.2021 – Plate 6 hours

	1	2	3	4	5	6	7	8	9	10	11	12
A	0.81	0.7698	0.8967	0.8396	1.0823	0.9325	0.8583	0.7745	0.7466	0.7357	0.7241	0.8293
B	0.7288	0.7384	0.9324	0.9697	0.3696	0.6667	0.8065	0.8881	0.7691	0.5938	0.5928	0.4937
C	0.7342	0.9327	1.0124	0.9315	1.4121	1.4823	1.0805	0.9826	1.0943	0.6476	0.6665	0.6446
D	0.8199	0.8321	0.9783	0.7663	0.7054	1.3984	1.0582	1.0802	1.2648	0.7896	0.8927	0.6497
E	1.4615	0.8009	0.9413	0.7591	0.8323	0.7398	0.7683	0.7653	0.7533	0.6899	0.7584	0.6813
F	0.7662	0.8095	0.975	0.7891	0.9547	0.7154	0.6281	0.7638	0.8962	0.5405	0.7168	0.4916
G	0.7896	0.7654	1.0388	0.9563	0.599	0.5111	1.054	0.546	0.5098	0.5848	0.6042	0.552
H	0.752	0.6735	0.7761	0.7127	1.1533	0.5643	0.5451	0.6015	0.5946	0.4141	0.4494	0.6213

Table 2.11 – Raw values, average values and standard deviation of PANC-1 metformin for 24 hours

	8000 µM	4000 µM	2000 µM	1000 µM	500 µM	250 µM	100 µM
Plate 26.3.21	0,6597	0,4391	0,5654	0,6132	1,4273	0,8697	0,6469
	0,8803	0,7679	1,3323	0,788	0,7358	1	0,38
	0,9142	0,1861	1,4367	0,7507	1,5637	1,2756	0,6598
Plate 9.4.21	1,8447	1,6308	1,6865	0,9998	0,8577	0,2038	1,1523
	1,9211	1,1734	1,4868	1,7292	1,0409	0,2302	1,1417
	1,052	0,6315	0,718	0,6386	1,6833	0,3054	1,1614
Average	1,212	0,9285	1,20428333	0,91991667	1,21811667	0,64745	0,95242
Standard deviation	0,53525267	0,522697358	0,45329852	0,4196597	0,39332336	0,45960419	0,33807525

Table 2.12– Raw values, average values and standard deviation of PANC-1 metformin for 6 hours

	8000 µM	4000 µM	2000 µM	1000 µM	500 µM	250 µM	100 µM
Plate 9.4.21	0,7288	0,7342	0,8199	1,4615	0,7662	0,7896	0,752
	0,7384	0,9327	0,8321	0,8009	0,8095	0,7654	0,6735
	0,93224	1,0124	0,9783	0,9413	0,975	1,0388	0,7761
Average	0,79981333	0,8931	0,87676667	1,0679	0,85023333	0,8646	0,73386667
Standard deviation	0,11478526	0,143265244	0,08814178	0,34802121	0,11019874	0,15134609	0,05364982

Table 2.13 – Raw values, average values and standard deviation of PANC-1 phenformin for 24 hours

	2000 µM	1000 µM	500 µM	250 µM	100 µM	50 µM	25 µM
	0,4642	0,7129	0,9845	0,6533	0,6436	0,8273	0,4809
Plate 26.3.21	0,4228	0,575	0,7173	0,9078	1,7679	1,1984	0,7866
	0,6066	0,6792	0,1848	0,5588	1,044	0,9219	0,1617
Plate 9.4.21	0,8105	0,7604	0,7128	0,7748	0,777	1,0167	1,1946
	0,8787	1,6758	0,7805	0,6182	0,7529	0,8006	1,3295
	1,2821	1,0096	1,9666	0,8591	0,8097	0,9379	1,488
Average	0,63656	0,90215	0,67598	0,72866667	0,96585	0,95046667	1,33736667
Standard deviation	0,17502008	0,449685354	0,29598559	0,13997685	0,41439873	0,14454191	0,14685811

Table 2.14 – Raw values, average values and standard deviation of PANC-1 phenformin for 6 hours

	2000 µM	1000 µM	500 µM	250 µM	100 µM	50 µM	25 µM
Plate 26.3.21	0,9797	0,9315	0,7663	0,7591	0,7891	0,9563	0,7127
	0,3696	1,4121	0,7054	0,8323	0,9547	0,599	1,1533
	0,6667	1,4823	1,3984	0,7298	0,7154	0,5111	0,5643
Average	0,672	1,2753	0,9567	0,77373333	0,81973333	0,6888	0,8101
Standard deviation	0,30508453	0,299801334	0,38373346	0,05279359	0,1225558	0,23579396	0,30634184

Table 2.15 – Raw values, average values and standard deviation of MIA PaCa metformin for 24 hours

	8000 µM	4000 µM	2000 µM	1000 µM	500 µM	250 µM	100 µM
Plate 26.3.21	3,3899	2,6757	2,6309	2,5742	1,8551	1,9739	1,9698
	2,8151	2,2203	2,291	2,5493	2,3704	1,6724	1,135
	2,8227	1,7309	2,7068	1,6143	2,23333	1,8563	1,5967
Plate 9.4.21	2,068	1,7815	0,7844	0,6145	0,6126	0,3089	2,566
	2,1007	0,2124	0,799	0,5945	0,6862	0,3418	2,926
	2,0614	1,591	0,1795	0,5846	0,6702	0,3862	1,5661
Average	2,542966667	1,99988	1,84242	1,4219	1,40463833	1,08991667	1,95993333
Standard deviation	0,551851964	0,83710049	0,9718808	0,96678856	0,83728361	0,821333	0,6735365

Table 2.16– Raw values, average values and standard deviation of MIA PaCa metformin for 6 hours

	8000 µM	4000 µM	2000 µM	1000 µM	500 µM	250 µM	100 µM
Plate 26.3.21	0,8065	1,0805	1,0582	0,7683	0,6281	1,054	0,5451
	0,8881	0,9826	1,0802	0,7653	0,7638	0,546	0,6015
	0,7691	1,0943	1,2649	0,7533	0,8962	0,5098	0,5946
Average	0,821233333	1,05246667	1,13443333	0,7623	0,7627	0,70326667	0,5804
Standard deviation	0,060852718	0,06089847	0,11352164	0,00793725	0,13405338	0,30428279	0,03076475

Table 2.17 – Raw values, average values and standard deviation of MIA PaCa phenformin for 24 hours

	2000 µM	1000 µM	500 µM	250 µM	100 µM	50 µM	25 µM
Plate 26.3.21	0,593	0,9758	2,1059	0,2124	1,437	1,6357	1,7127
	0,5932	2,146	2,5332	2,699	2,1363	2,048	2,1702
	0,6242	1,4062	1,7299	2,1227	1,9368	2,2431	2,4543
Plate 9.4.21	2,5091	2,7792	2,9369	1,5297	1,0283	0,6654	1,8562
	2,3998	2,4184	2,3335	1,9065	0,6807	0,6726	1,3156
	1,6018	1,7733	2,1042	1,2899	1,0508	0,8458	2,0796
Average	1,38685	1,91648333	2,2906	1,6267	1,37831667	1,35176667	1,93143333
Standard deviation	0,913611453	0,66553046	0,41512466	0,84820034	0,56680401	0,71389116	0,39625937

Table 2.18 – Raw values, average values and standard deviation of MIA PaCa phenformin for 6 hours

	2000 µM	1000 µM	500 µM	250 µM	100 µM	50 µM	25 µM
Plate 26.3.21	0,5938	0,6476	0,7896	0,6899	0,5405	0,5848	0,4141
	0,5928	0,6665	0,8927	0,7584	0,7168	0,6042	0,4494
	0,4937	0,6446	0,6497	0,6813	0,4926	0,552	0,6213
Average	0,5601	0,6529	0,77733333	0,70986667	0,5833	0,58033333	0,49493333
Standard deviation	0,057506261	0,01187308	0,12196353	0,04225048	0,11806901	0,0263851	0,11085091

3. Flow cytometry
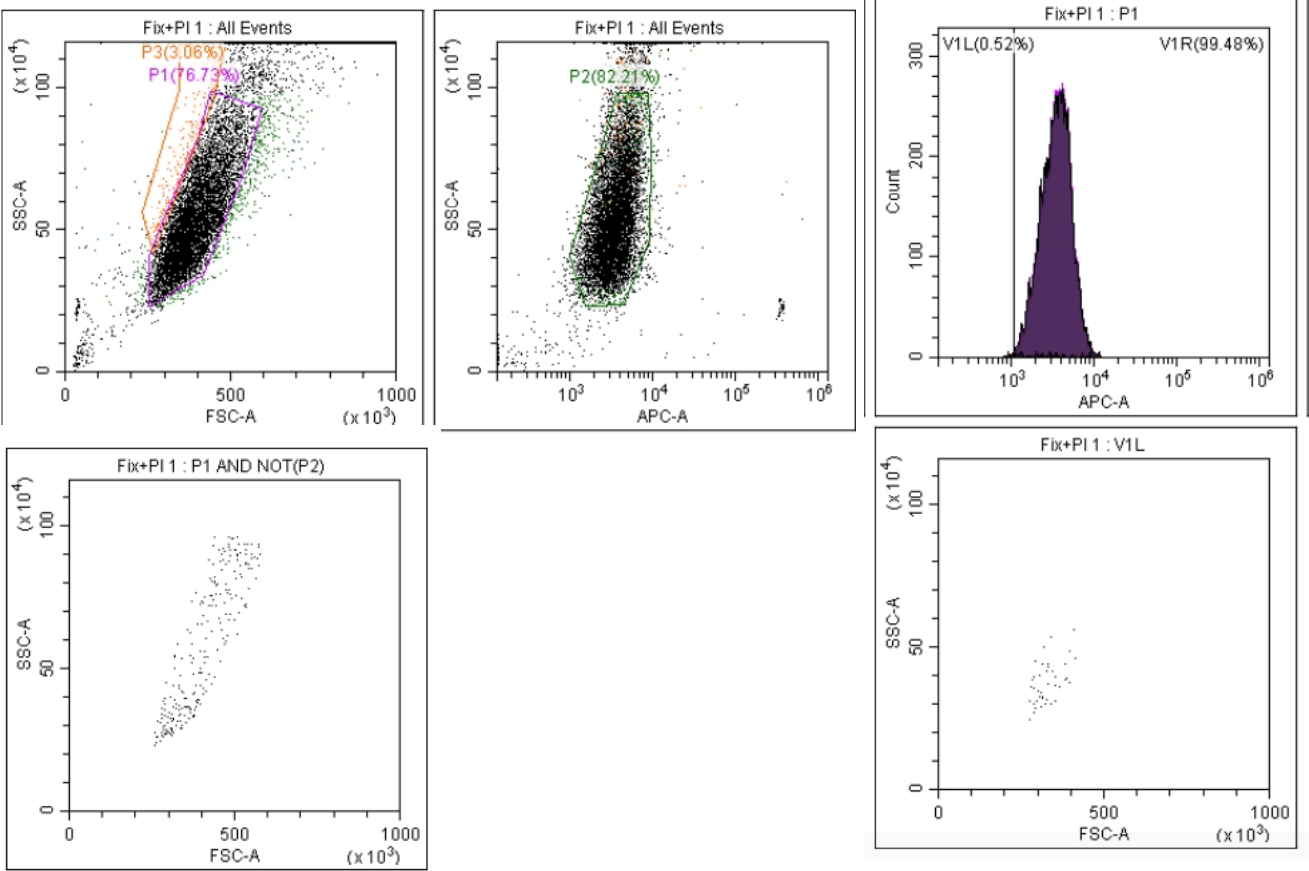
Figure 3.1 – Schematic overview with dot plots and histogram for optimalization of fixated MIA PaCa-2 cells with PI
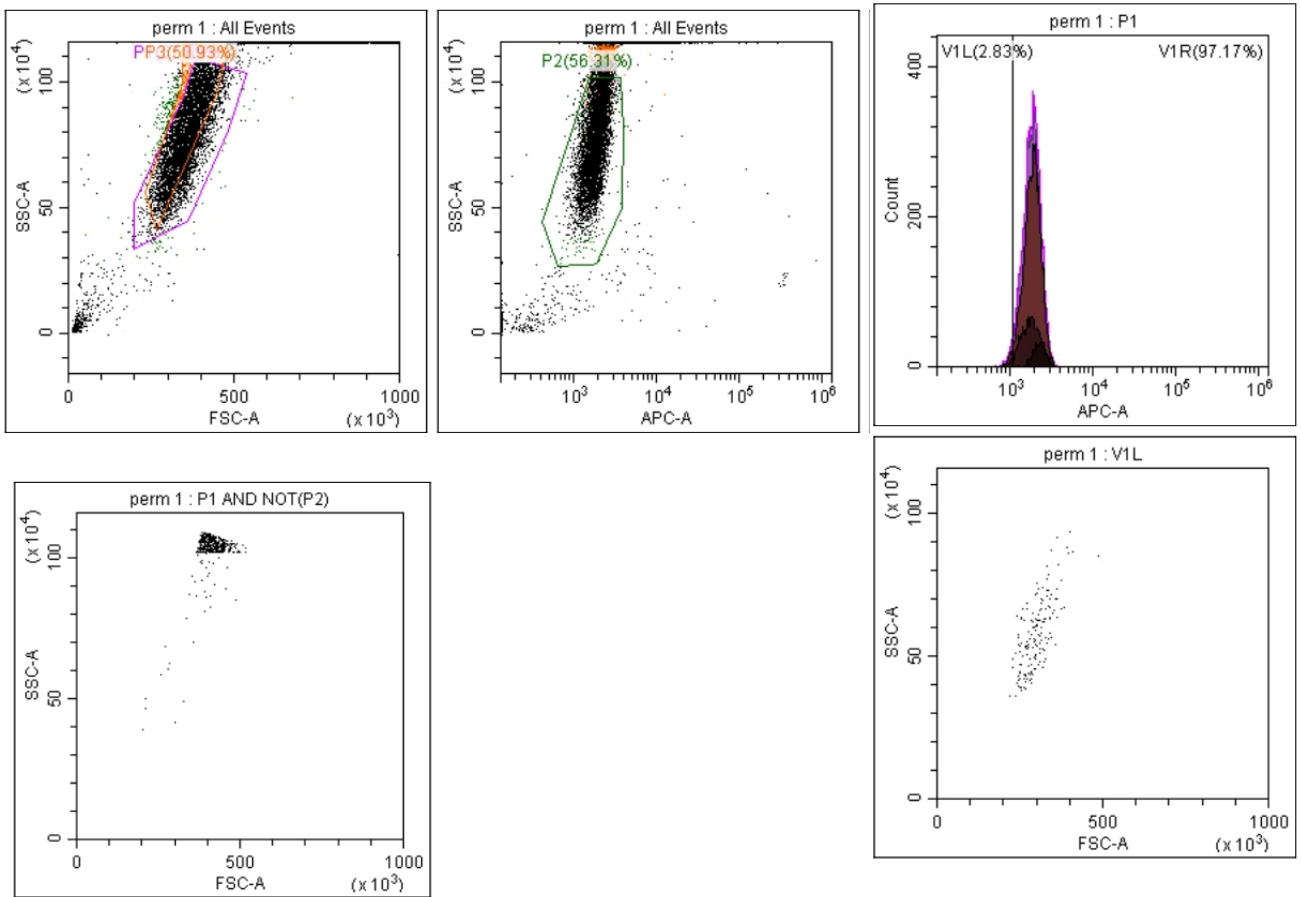
Figure 3.2 – Schematic overview with dot plots and histogram for optimalization of permeabilized MIA PaCa-2 cells
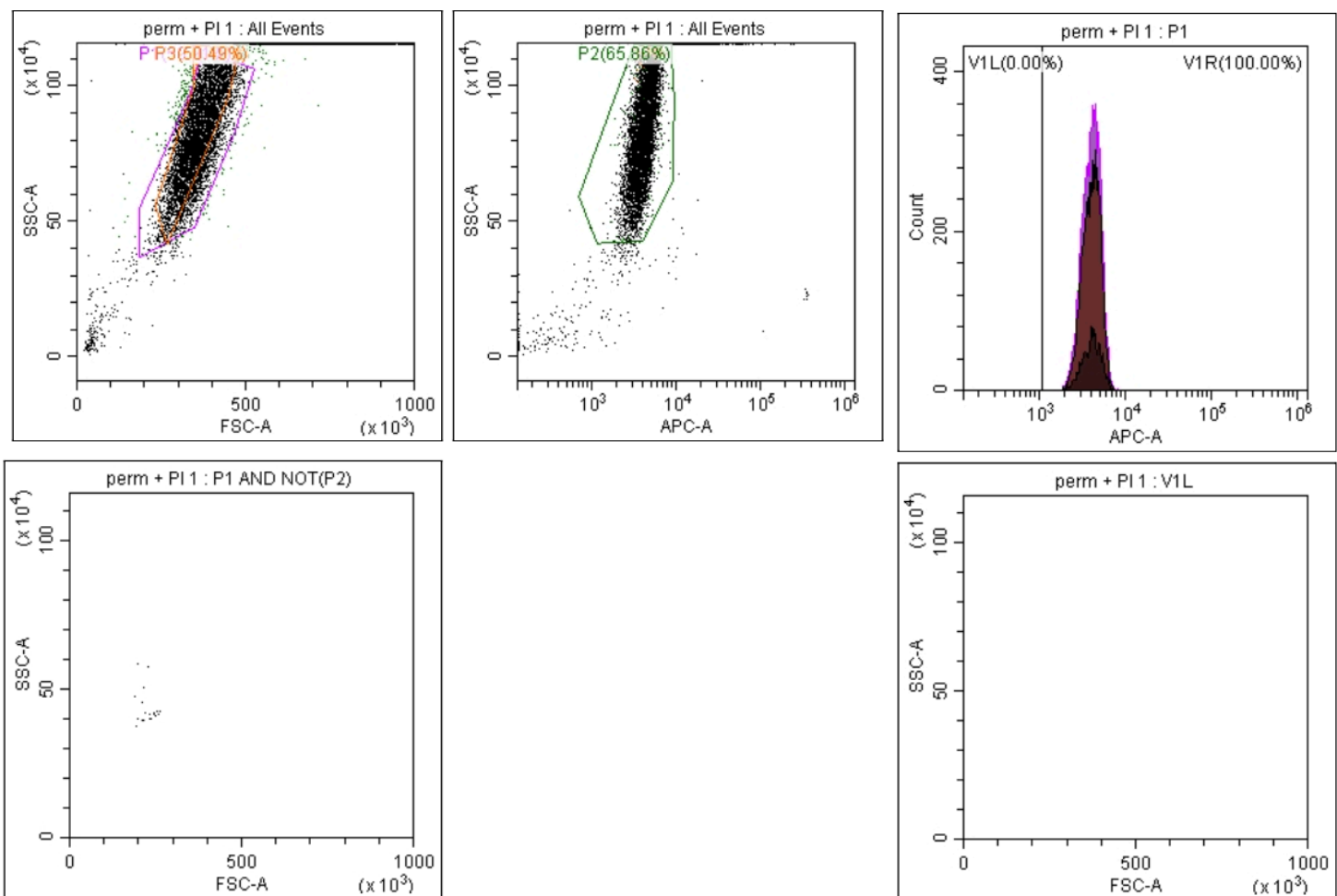
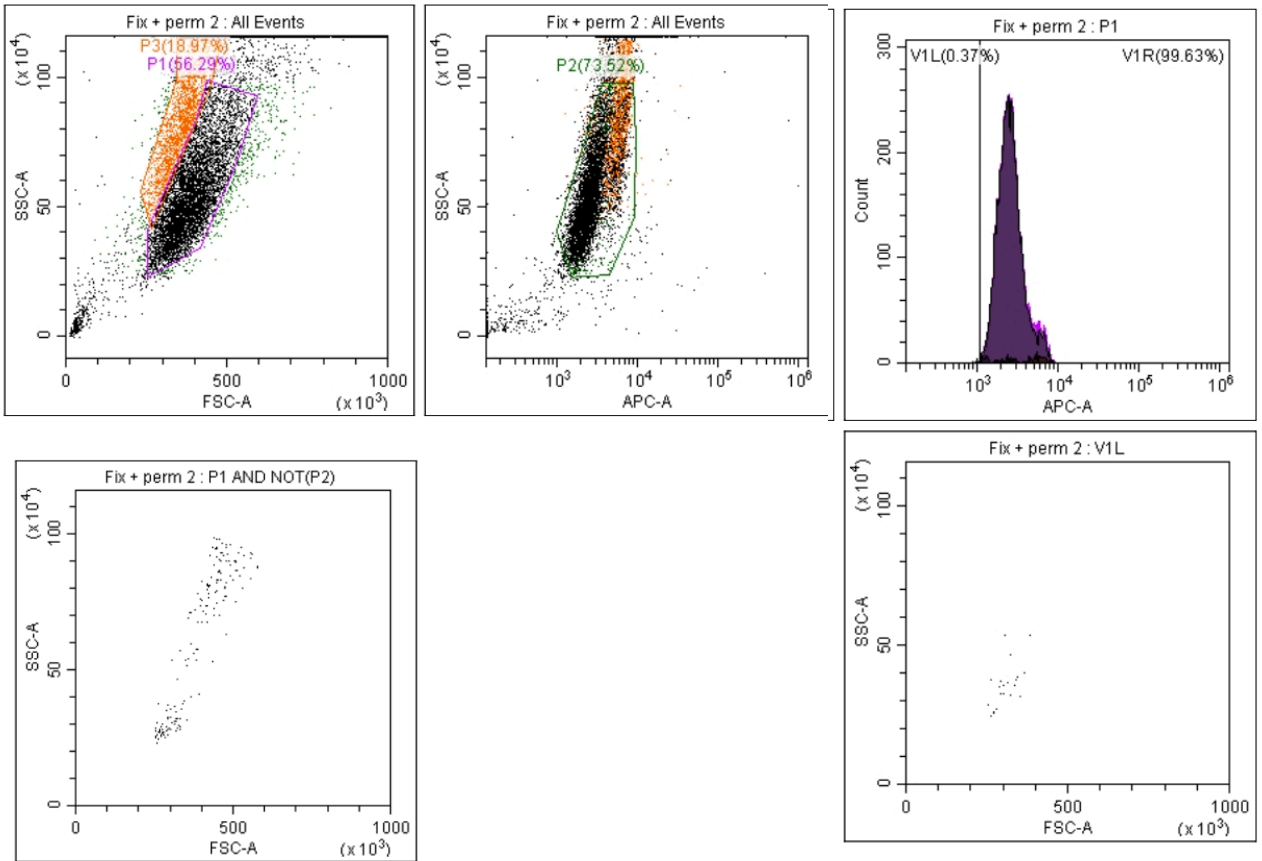*Figure 3.3 – Schematic overview with dot plots and histogram for optimalization of permeabilized MIA PaCa-2 cells with PI*

Figure 3.4 – Schematic overview with dot plots and histogram for optimalization of equal mix of fixated and permeabilized MIA PaCa-2 cells
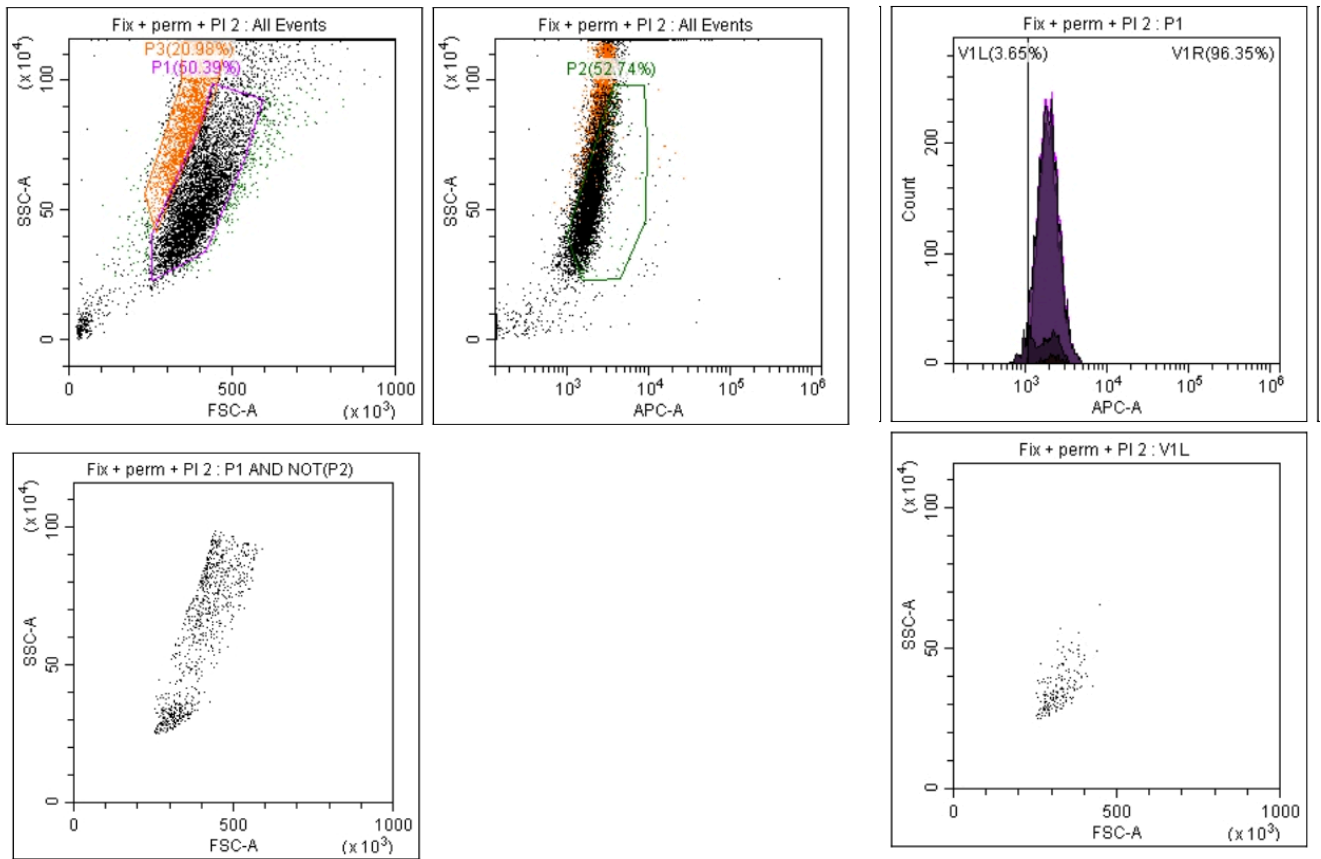
Figure 3.5 – Schematic overview with dot plots and histogram for optimalization of equal mix of fixated and permeabilized MIA PaCa-2 cells with PI